Molecular Imaging of Tuberculosis

Ismaheel O. Lawal MBBS, PhD[1,2]; Sofiullah Abubakar MBBS, MMED[3]; Alfred O. Ankrah MD, PhD[2,4,5]; Mike M. Sathekge MD, PhD[2,6]

1. Division of Nuclear Medicine and Molecular Imaging, Department of Radiology and Imaging Sciences, Emory University, Atlanta, GA, United States
2. Department of Nuclear Medicine, University of Pretoria, Pretoria, South Africa
3. Department of Radiology and Nuclear Medicine, Sultan Qaboos Comprehensive Cancer Care and Research Center, Muscat, Oman
4. National Center for Radiotherapy Oncology and Nuclear Medicine, Korle Bu Teaching Hospital, Accra, Ghana
5. Medical Imaging Center, Department of Nuclear Medicine and Molecular Imaging, University Medical Center Groningen, Groningen, The Netherlands
6. Nuclear Medicine Research Infrastructure (NuMeRI), Steve Biko Academic Hospital, Pretoria, South Africa

Corresponding author

Ismaheel O. Lawal, MBBS, PhD

Department of Radiology and Imaging Sciences

Emory University

1364 Clifton Rd., NE

Atlanta, GA 30322

Telephone: 1 404-712-1348

Email: ilawal@emory.edu

Abstract

Despite the introduction of many novel diagnostic techniques and newer treatment agents, tuberculosis (TB) remains a major cause of death from an infectious disease worldwide. With about a quarter of humanity harboring *Mycobacterium tuberculosis* (MTB), the causative agent of TB, the current efforts geared towards reducing the scourge due to TB must be sustained. At the same time, newer alternative modalities for diagnosis and treatment response assessment are considered. Molecular imaging entails the use of radioactive probes that exploit molecular targets expressed by microbes or human cells for imaging using hybrid scanners that provide both anatomic and functional features of the disease being imaged. Fluorine-18 fluorodeoxyglucose (FDG) is the most investigated radioactive probe for TB imaging in research and clinical practice. When imaged with positron emission tomography interphase with computed tomography (PET/CT), FDG PET/CT performs better than sputum conversion for predicting treatment outcome. At the end of treatment, FDG PET/CT has demonstrated the unique ability to identify a subset of patients declared cured based on the current standard of care but who still harbor live bacilli capable of causing disease relapse after therapy discontinuation. Our understanding of the pathogenesis and evolution of TB has improved significantly in the last decade, owing to the introduction of FDG PET/CT in TB research. FDG is a non-specific probe as it targets the host inflammatory response to MTB, which is not specifically different in TB compared with other infectious conditions. Ongoing efforts are geared towards evaluating the utility of newer probes targeting different components of the TB granuloma, the hallmark of TB lesions, including hypoxia, neovascularization, and fibrosis, in TB management. The most exciting category of non-FDG PET probes developed for molecular imaging of TB appears to be radiolabelled anti-tuberculous drugs for use in studying the pharmacokinetic characteristics of the drugs. This allows for the non-invasive study of drug kinetics in different body compartments concurrently, providing an insight into the spatial heterogeneity of drug exposure in different TB lesions. The ability to repeat molecular imaging using radiolabelled anti-tuberculous agents also offers an opportunity to study the temporal changes in drug kinetics within the different lesions during treatment.

Keywords: Molecular imaging, FDG PET/CT, Tuberculosis, Tuberculous granuloma, Fever of unknown origin, Anti-tuberculous treatment, Residual metabolic activity

1. Introduction

Prior to the emergence of severe acute respiratory syndrome coronavirus-2 (SARS-CoV-2), *Mycobacterium tuberculosis* (MTB), the agent of tuberculosis (TB), was the single pathogen responsible for the largest proportion of death from infectious diseases among humans. About a quarter of humanity (1.7 billion people) are infected with MTB [1]. About 5-15% of these infected populations will develop TB disease at some point in their lifetime [2]. While the risk of developing clinically overt TB disease is highest within the first 12 to 18 months of acquiring the infection, reactivation of this latent infection can occur decades later [3]. Conditions causing impaired innate or acquired host immunity are the most important predisposing factors to TB reactivation. Infection with human immunodeficiency virus (HIV) is a common disorder predisposing to TB reactivation, making TB one of the most frequently encountered opportunistic infections in HIV-infected patients. Other conditions that predispose to the reactivation of latent TB infection include malnutrition, diabetes mellitus, chronic renal failure, smoking, occupational lung diseases such as silicosis, and treatment with immunosuppressive therapies such as tumor necrosis factor-alpha (TNF-α) inhibitors [3-5].

Timely diagnosis is vital to preventing morbidity and mortality associated with TB. There are several tools available for TB diagnosis [6]. The time-tested, cheap, readily available sputum microscopy using the Ziehl-Neelsen staining technique offers a rapid diagnosis of TB and allows for quantifying bacillary load. Sputum microscopy, unfortunately, has low sensitivity, especially in patients with paucibacillary TB, and may be falsely negative at a bacillary load below 10,000 bacilli/mL of sputum [6]. Detection is improved by fluorescent microscopy using the auramine-rhodamine staining technique. Culture using liquid or solid media has better sensitivity for MTB detection than microscopy, but it is time-consuming, requiring weeks to obtain a positive culture [7,8]. Xpert MTB/RIF and Xpert MTB/RIF Ultra are nucleic acid amplification tests recommended by the World Health Organization (WHO) for diagnosing TB in children and adults, including patients with HIV infection. They offer rapid and automated detection of MTB and rifampicin resistance in biological samples [9]. Despite this array of diagnostic tools available to clinicians, a substantial fraction of patients with TB is treated empirically due to the failure to isolate MTB on microbiological or molecular testing. In a series from a TB endemic region, positive culture was obtained in only 30% of patients treated for TB [10]. Imaging is, therefore, used as a supporting tool in TB diagnostics. A chest radiograph is the most used imaging technique due to its availability and low cost. Chest radiographs perform poorly when used for TB diagnosis and have not been found to improve the performance of Xpert MTB/RIF [11,12].

Computed tomography (CT) has better sensitivity for lesion detection than planar chest radiograph. The severity of lung lesions induced by pulmonary tuberculosis (PTB) directly correlates with bacillary load [13,14]. The application of molecular imaging techniques in TB imaging dates back to the 70s with single-photon emitting radionuclides such as Gallium-67 citrate [15]. In the years that followed, many studies reported the clinical utility of planar and single-photon emission tomography (SPECT) imaging techniques in the detection of TB, its differentiation from other pathologies, and its response to anti-tuberculous treatment [16-19]. The clinical application of scintigraphy with single-photon emitting radiopharmaceuticals has dwindled significantly since the introduction of positron emission tomography (PET) into the clinics in the early 2000s. PET has a high sensitivity for lesion detection at nanomolar target concentration, and its quantification capability makes it a valuable modality for prognostication and treatment response assessment. Fluorine-18 Fluorodeoxyglucose (FDG), a glucose analog, is the commonest radiopharmaceutical for PET imaging. PET, now interphase with CT for hybrid imaging, makes whole-body FDG PET/CT a modality for the holistic

assessment of pulmonary and extrapulmonary TB. Several original studies done in different settings have reported the utility of PET/CT for the initial assessment, prognostication, response assessment, and prediction of relapse of TB. Two articles appearing in an issue of this journal published about five years ago performed a comprehensive review of the studies [20,21]. Since the publication of these two articles, several original articles have been published in the literature advancing the frontiers of knowledge regarding novel clinical applications and the potential of molecular imaging techniques in pulmonary and extrapulmonary TB. This current work, therefore, serves to present an updated appraisal of the literature on the applications of radionuclide techniques in molecular imaging of TB.

2. The Tuberculous Granuloma at the Crux of the Matter

The tubercle bacilli are airborne, making PTB, by far, the commonest form of TB. Following inhalation into the alveoli, the bacilli are phagocytosed by alveolar macrophages. MTB inhibits the maturation of phagosome by inhibiting its fusion with lysosome [22]. MTB, therefore, replicates uncontrollably within macrophages. After a few weeks of unchecked replication within macrophages, MTB antigen is presented to naïve T helper cells in association with interleukin-12 (IL-12) in the draining lymph nodes. This causes the naïve T-helper cells to differentiate into T-helper 1 cells, which in turn secrete interferon-gamma (IFN-γ) [23]. IFN-γ plays a central role in host immune response against MTB by stimulating the maturation of phagolysosomes capacitating macrophages to destroy engulfed bacilli, inducing the production of soluble anti-mycobacterial factors including defensins, and causing the formation of granuloma and caseous necrosis [24]. Under the influence of IFN-γ, macrophages transform into epithelioid cells, some of which coalesce to form multinucleated Langhans giant cells [25]. The TB granuloma, therefore, consists of infected and uninfected epithelioid cells, foamy macrophages, multinucleated giant cells, and a surrounding fibroblastic cuff interspersed with lymphocytes (figure 1). At the core of the granuloma is the cheesy necrosis that characterizes the caseous necrosis of tuberculous granuloma. Activated macrophages secrete tumor necrosis factor (TNF) and other chemokines that recruit more macrophages, B and T cells, neutrophils, natural killer (NK) cells, and fibroblasts to maintain the integrity of the granuloma [26,27]. In most patients, the granuloma so formed can curtail the infection resulting in latent tuberculosis. In a small proportion of infected patients, this primary infection leads to primary progressive disease that is symptomatic [25]. Secondary tuberculosis occurs when a breakdown in the host immune system occurs later, compromising the integrity of the tuberculoma. Dissemination of the hitherto sequestered MTB bacilli via the lymphatic and hematogenous routes leads to extrapulmonary tuberculosis (EPTB).

The tuberculoma plays the dynamic role of curtailing the systemic dissemination of mycobacterial and providing a niche for their persistence at the same time [28]. To the imager, the allure of the tuberculoma is the possibility of exploring the different targets expressed by the various cellular and pathologic components of the tuberculoma for molecular imaging of TB. This dynamism afforded by molecular imaging techniques makes the characterization of the biological behavior and metabolic pathways that drive diseases, including TB, possible [29,30].

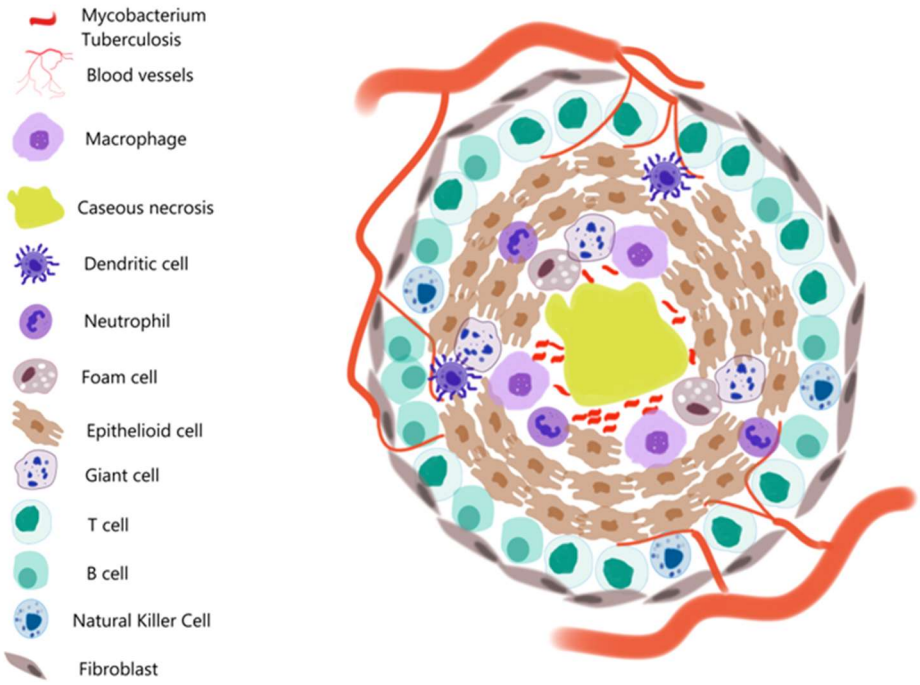

Figure 1: A schematic diagram of the tuberculous granuloma. The granuloma consists of an abundance of different forms macrophages including epithelioid cells, giant cells, and foam cells. Interspersed between these macrophages are neutrophils and dendritic cells. The granuloma is surrounded by a lymphocytic cuff. At the core of the granuloma is the central area of caseous necrosis. In lung standing granulomas, a peripheral rim of fibroblast producing fibrotic changes may be seen.

3. Radionuclide Imaging of Tuberculosis: The Possibilities

Radionuclide imaging techniques have been applied in interrogating the various aspects of Tb, including disease diagnosis, lesion characterization, disease evolution, treatment response assessment, prognostication, relapse prediction, and pharmacokinetic study of current and novel anti-TB drugs [20,21,31,32]. This array of applications of radionuclide imaging techniques explored in studying TB infection and disease in humans and laboratory animals has advanced the knowledge regarding the disease. In this section, we will discuss the applications of radionuclide techniques in the clinical imaging of TB and EPTB while drawing mechanistic evidence from relevant preclinical studies. By far, PET/CT is the more common radionuclide technique applied in TB imaging. Hence, our discussion will mainly focus on published evidence regarding its use in TB imaging. The granuloma is the hallmark feature of the TB lesion. The TB granuloma is packed with activated inflammatory cells, which increase their consumption of metabolic substrates, including glucose, to cope with the metabolic demand of the intense inflammation that accompanies TB. FDG, therefore, has a wide range of applications in TB. Other tracers exploring other metabolic pathways or more specific targets expressed by inflammatory cells have also been studied in TB. More recently, radiolabeled anti-TB drugs have been explored for PET-based pharmacokinetic studies to determine drug concentration in healthy and disease tissues. These non-FDG PET tracers will be discussed in later sections.

3.1. FDG PET/CT as an ancillary tool for TB diagnosis

Pulmonary TB

Identifying MTB in biological samples is necessary for a definitive diagnosis of TB. PET/CT imaging, therefore, plays an ancillary role, useful for TB diagnosis only when obtaining the requisite biological sample is not feasible or when there is a failure of MTB identification from biological samples. Also, TB lesions may be seen on the images of patients without overt TB symptoms imaged for other indications. For these reasons, the interpreting physicians must be familiar with the appearance of TB on clinical PET/CT images. Soussan et al. described two patterns of pulmonary lesions due to PTB on FDG PET/CT images; the lung and the lymphatic patterns [33]. The patients with the lung pattern of PTB lesions have pulmonary symptoms and associated pulmonary parenchyma lesions on FDG PET/CT, including focal or multifocal FDG uptake in regions of lung consolidation with or without cavitations, surrounded by micronodules. In the lung pattern of PTB, pathological lymph nodes are only slightly enlarged and show moderate FDG avidity (maximum standardized uptake value, SUVmax of 2.5 – 13.3). PTB is usually the source of MTB dissemination to distant sites causing EPTB. Some patients with the lung pattern of PTB may, therefore, have extrapulmonary lesions due to EPTB. In the lymphatic pattern, systemic symptoms such as fever predominate, and extrapulmonary sites of disease involvement are more common. In the small series by Soussan et al., the sites of EPTB involvement were extra-thoracic lymph nodes, liver, spleen, and peritoneum [33]. The lymphatic pattern of disease is associated with larger thoracic nodes with more intense FDG avidity compared with the lung pattern. Lung lesions, when present in the patients with the lymphatic disease pattern, may demonstrate a miliary pattern or ground-glass opacities [33]. This categorization was described based on data from a study with a modest study population. Yes, it provides an insight into the dynamic nature of TB, a dynamism driven by both pathogen-related and host immune-related factors. The lung pattern may suggest MTB disease in a host with a robust immunity that reduces the systemic dissemination of the pathogen, while the lymphatic pattern may suggest a more florid infection in a patient without robust host immunity against the spread of the infection. The validity of the classification, its impact on response to anti-tuberculous treatment, and its long-term prognosis need to be confirmed in larger studies. Figure 2 shows the FDG PET/CT images of a patient in which imaging findings prompted the investigation for PTB.

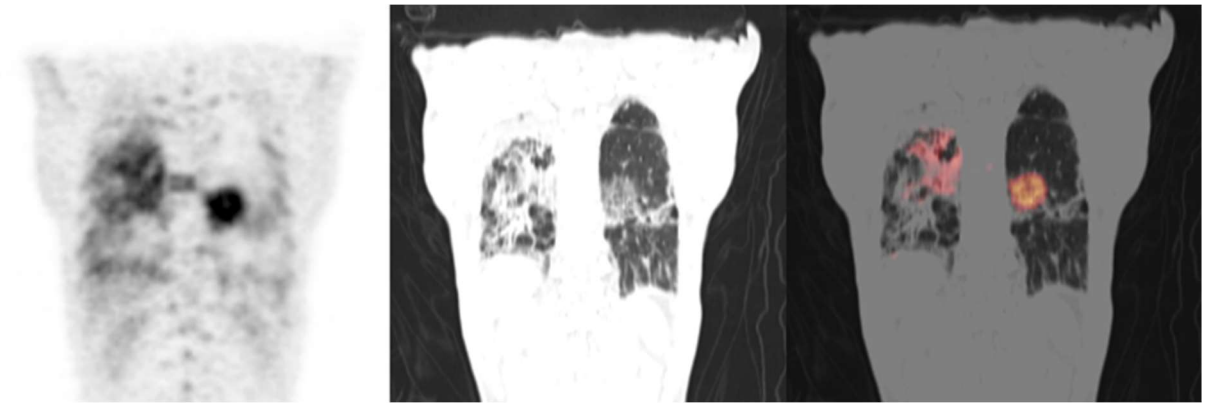

Figure 2: Tuberculosis reactivation caused by chemotherapy-induced immunosuppression. A 47-year-old male developed new-onset fever, cough and dyspnoea while undergoing chemotherapy for Hodgkin lymphoma. FDG PET/CT scan was obtained as part of his work-up. Images show FDG-avid lesions in the lungs bilaterally. Diffusely increased bone marrow FDG uptake is seen consistent with bone marrow reactivation caused by anaemia induced by chemotherapy. Pulmonary tuberculosis was confirmed as the cause of the lung lesions following a positive sputum culture for Mycobacterium tuberculosis. This case highlights the role of immunosuppression induced by cancer chemotherapy in the reactivation of latent tuberculous infection.

Extra-pulmonary TB

FDG PET/CT may play a more significant role in EPTB than in PTB because of the challenges associated with obtaining a definite diagnosis in the former compared with the latter. The biggest challenge against establishing a definitive diagnosis (isolation of tubercle bacilli) relates to the difficulty in obtaining the biological sample necessary for tissue, microbiological or molecular testing. This may be due to the absence of localizing symptoms or disease localization to body parts that may be considered too risky for invasive biopsies, such as the brain and spinal cord [34]. When obtained, the biological sample may have a poor yield for the isolation of the tubercle bacilli, such as with cerebrospinal fluid (CSF) in the evaluation of patients with suspected tuberculosis of the central nervous system (CNS) [34,35].

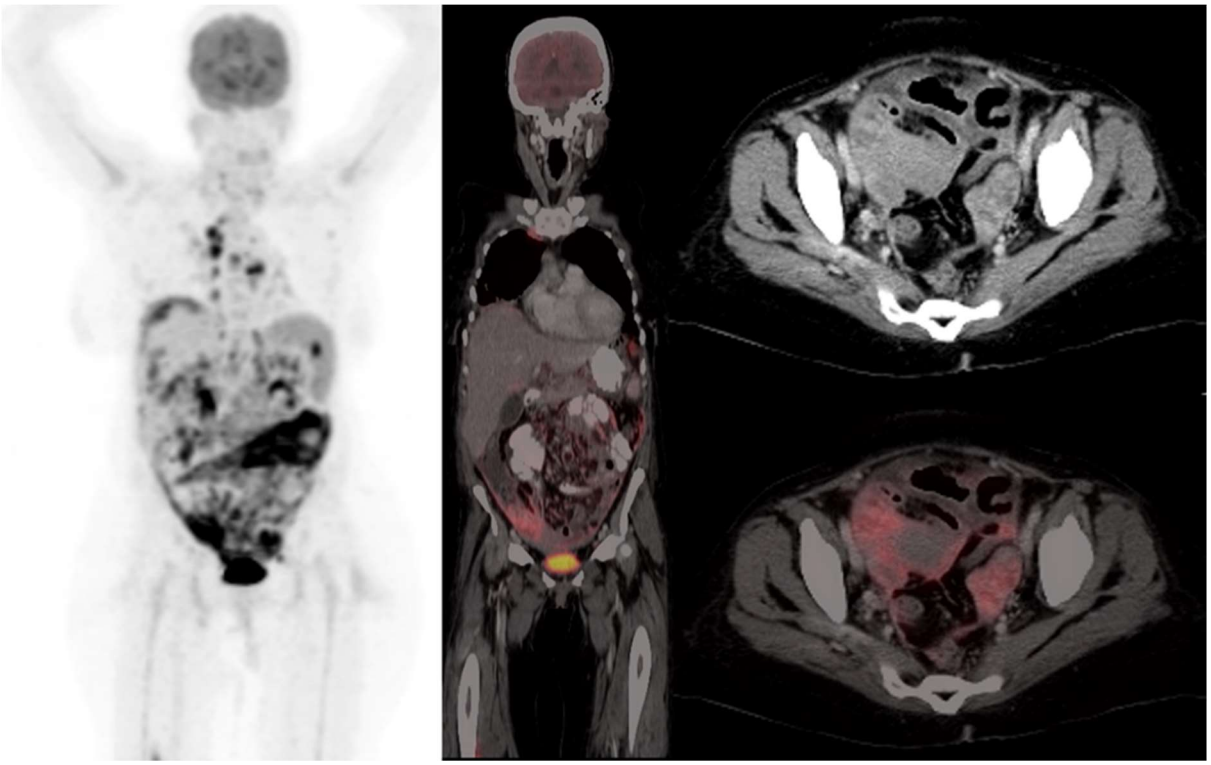

Figure 3: FDG PET/CT images of a middle-aged woman with pulmonary tuberculosis. On account of abdominal symptoms and associated ascites, FDG PET/CT was obtained to evaluate for extra-pulmonary sites of disease involvement. In addition to the FDG-avid chest lesions, there is thickening of peritoneum with intense FDG uptake suggestive of concomitant peritoneal tuberculosis. Ascites and abdominal symptoms resolve with anti-tuberculous treatment. This case highlights the role of FDG PET/CT to evaluate the whole-body burden of the disease.

Some small single-center studies have reported the utility of FDG PET/CT for imaging extrapulmonary tuberculosis. Recently, a large multicentre international study reported the clinical utility of FDG PET/CT in 358 HIV-negative patients with EPTB [36]. In 350 patients, at least one site of increased FDG uptake suggestive of EPTB was seen (one site of extrapulmonary disease in 118 patients and two or more sites of extrapulmonary disease in 232), giving FDG PET/CT an overall sensitivity of 98% for lesion detection. The commonest sites of disease involvement were in the lymph nodes (n=225), bones (n=151), brain (n=34), and pleura (n=34). In the eight patients categorized as having negative FDG PET/CT, lesions with low-grade FDG avidity (SUVmax < 2.5) suggestive of TB were seen in the leptomeninges (n=2, one of whom had associated brain

parenchyma lesion), bones of the spine and pelvis (n=4), and abdomen (ascites and thickened omentum, n=2). Interestingly, 100 patients showed concomitant pulmonary lesions suggestive of PTB. There was no clinical suspicion of concomitant PTB in 28 of these 100 patients referred to FDG PET/CT for assessing EPTB [36]. Put together, this study shows the utility of FDG PET/CT to detect EPTB at various sites within the body, its ability to detect disease at previously unknown sites of EPTB involvement, and its utility in quantifying the whole-body disease burden (figure 3). These additional pieces of information available from FDG PET/CT may have therapy implications as disease involvement at some sites may require longer treatment than the six-month treatment duration generally offered to PTB and some sites of EPTB disease.

TB presenting as fever of unknown origin

TB is the largest contributor to infectious causes of fever of unknown origin (FUO) across many regions of the world, including Europe [37]. The diagnostic contribution of FDG PET/CT to the unraveling of the cause of fever in different groups of patients with FUO has been well reported [38-40]. Applying FDG PET/CT in patients presenting with FUO may, therefore, aid in unraveling TB as the cause of prolonged fever. TB reactivation is especially seen in the context of immunosuppression. The diagnostic yield of FDG PET/CT for TB as the cause of fever may consequently be higher in patients with immunosuppression.

HIV infection is an immunosuppressive disease that increases the risk of latent TB reaction as well as the development of primary progressive disease following newly acquired infection [41,42]. In a small study of 10 HIV-infected patients who had FDG PET/CT for the evaluation of FUO, the scans of nine patients were positive, six patients with TB and three patients with neoplasms [43]. In a larger prospective study from the same group of authors, including 20 HIV-infected patients with FUO all of whom had positive FDG PET/CT scan findings, MTB and non-tuberculous mycobacteria were the causes of fever in 8 and 3 patients, respectively [44]. These studies included HIV-infected patients not on antiretroviral therapy (ART). While patients' immune status improves considerably while on ART, the risk of acquiring new TB disease or reactivation of latent TB is always higher than in the HIV-negative population [42]. The findings from these studies are, therefore, still applicable in the current era where all persons living with HIV infection are treated with ART regardless of their CD4 T-cell count.

End-stage renal disease (ESRD) is another immunosuppressive condition that increases the risk of TB reactivation [45]. Among patients with ESRD, TB presents as FUO in up to 77% of patients [46]. Two recent studies have evaluated the diagnostic role of FDG PET/CT in patients with ESRD presenting with FUO [47,48]. In one study of 20 patients, FDG PET/CT helped unravel the cause of fever in 15 patients. Fifteen patients were eventually treated for tuberculosis, underscoring the prevalence of TB as the cause of FUO among the patients [47]. In the second study that included 47 patients, 22 of whom had positive findings on FDG PET/CT all due to infectious aetiologies, TB was the cause of fever in four patients (three with TB lymphadenitis and one with PTB) [48]. Both studies show that FDG PET/CT can significantly contribute to the localization of the cause of fever in patients with end-stage renal disease presenting with FUO and point to TB as an important etiology to be considered.

Limitations of FDG PET/CT in the diagnosis of TB

FDG is trapped significantly by the activated inflammatory cells present in TB granuloma, causing an intense FDG uptake in TB lesions and a high yield of FDG PET/CT in the diagnostic workup of patients. Unfortunately, neither the pattern nor the intensity of FDG uptake, on their own, is sufficient to diagnose PTB or EPTB based on FDG PET/CT. Many attempts have been made to

improve the discriminative power of FDG PET/CT in differentiating TB from other conditions such as neoplasms and non-tuberculous infections. In the lungs, for example, dual-time-point FDG PET/CT imaging has not been consistent in differentiating solitary lung nodules due to malignancy versus TB or other benign inflammatory conditions [49-51]. Other scenarios in which studies have evaluated the diagnostic ability of FDG PET/CT for TB and its differentiation from related conditions include PTB versus bacterial infections [52], tuberculous versus non-tuberculous mycobacterial disease [53], pleural TB versus mesothelioma [54], peritoneal TB versus peritoneal carcinomatosis [55,56], and TB spondylodiscitis versus pyogenic spondylodiscitis [57]. Dual-time-point imaging has also been explored in differentiating pyogenic from TB spondylodiscitis [58]. In some of these studies, FDG PET/CT performed poorly in differentiating between TB and other conditions, while in some others, notable differentiating features were identified to discriminate between TB and other conditions. Overall, the strength of the evidence available for each of the comparisons is not enough to allow for patient treatment based on imaging findings alone. This does not negate the benefits of FDG PET/CT as an ancillary tool in diagnosing PTB and EPTB, but emphasizes the importance of molecular, microbiological, or tissue diagnosis to reach a definitive diagnosis. When these testings are not feasible or do not return positive for MTB, there is a role for empirical treatment based on imaging findings, suggestive clinical findings, and other supportive biomarkers. Importantly, findings on FDG PET/CT may serve as a guide for biopsy to obtain tissue for microbiological diagnosis.

3.2. Understanding the evolution of TB lesions: The contribution of FDG PET/CT

TB is one of the oldest diseases known to man. Nevertheless, much remains to be understood regarding the factors responsible for the different pathways TB infection may take in different individuals. Even in the same individual, different TB relations have different biological behaviors before, during, and after treatment. Early TB works were based on human autopsy studies. With the advent of effective anti-tuberculous treatment (ATT), mortality due to TB reduced significantly, and so did the use of tissue samples obtained at autopsy for TB study. Murine models were subsequently employed in the study of TB. Many mice models of TB do not form the complex lesions characteristic of human TB. For example, mice models of TB do not always form caseous necrosis or cavitary lesions [59]. TB lesions seen in rabbits and nonhuman primates closely resemble those of humans and are now more commonly used as surrogates of human TB. The exquisite sensitivity of PET and the detailed anatomic information provided by CT have made FDG PET/CT a very useful tool for TB study in experimental animals. The fact that FDG PET/CT imaging is non-invasive and repeated imaging can be obtained in the same experimental animals has made this imaging modality an attractive, cost-effective means of gaining insights into the in vivo biology of TB in experimental animals and humans.

In patients presenting with suggestive symptoms, sputum samples are collected to detect MTB. In a pilot active case-finding study from South Africa, 20 patients with one or more symptoms of PTB were made to wear a face mask for 30 minutes, followed by sputum collection [60]. 12/20 patients had negative face masks and sputum for MTB. On follow-up for ten months, none of these 12 patients developed TB. 8/20 patients had positive detection of MTB, including six patients in whom MTB was detected in their face masks alone and not in their sputa. FDG PET/CT obtained in the patients with MTB detection in their face mask only showed radiotracer-avid lesions, including pulmonary nodules and tree-in-bud changes consistent with TB-induced bronchiolitis. The sputa of four of five patients (one was lost to follow-up) became positive for MTB during follow-up [60]. This small and simple study is revealing, showing that suggestive lung lesions may precede sputum positivity, and these lesions due to PTB are detectable by FDG PET/CT.

Some important studies utilizing FDG PET/CT for imaging TB in cynomolgus macaques and rabbits have advanced our understanding of the dynamism of TB granulomas from their formation following infection acquisition to the establishment of active or latent infection and the behavior of granulomas that are at increased risk of reactivation following immunosuppression [61-65]. Following exposure to MTB, the fate of the infection ranges from active TB disease, latent disease, or a disease phenotype characterized by the absence of active disease but persistent culture positivity of the respiratory samples, the so-called percolators [61,63]. Discrete granulomas with avidity for FDG are established in the lungs as early as three weeks post-infection acquisition with no significant difference in the number, size, and FDG avidity of the granulomas of animals destined to result in active TB versus latent TB infection [61]. These early granulomas are generally located in the lower lobes, but their locations vary by the mechanism of infection, endobronchial instillation versus aerosolization [62]. Between 3- and 6-weeks post-infection, the behavior of granulomas in animals that developed active TB differs significantly from those that developed a latent infection. Granulomas in animals that developed active TB generally increased in number, size, and FDG avidity. In contrast, granulomas of animals that developed latent infection may remain stable in number but show heterogeneity in FDG avidity (avidity may remain the same, increase or decrease compared with the level at week 3) [61,63].

The mediastinal lymph nodes play important roles in the pathogenesis of TB as they are an important site for T-cell priming and trafficking while also serving as a reservoir of bacilli responsible for TB reactivation [66]. Mediastinal lymph node involvement in early TB may occur without a significant increase in size to meet CT criteria for pathologic lymph node. They, however, demonstrate FDG avidity making FDG PET a sensitive tool for their evaluation in early TB infection [61,63]. All animals, regardless of the fate of infection (active or latent), demonstrate metabolically active mediastinal lymph nodes reflecting the role these nodes play in host immunity against TB and their early involvement in the course of the infection. Unlike lung granulomas, the mediastinal lymph nodes are less dynamic during the first three months of infection, with a similar number of nodes seen in animals that develop active versus those that develop a latent infection. The FDG avidity is a better discriminator, showing higher intensity in active-disease animals compared with passive-disease animals [61].

The early granulomas are generally solid, consisting of histiocytes and neutrophils surrounded by a rim of lymphocytes. Over time, cavities appear in the center of the granulomas consisting of epithelioid macrophages and rare multinucleated giant cells surrounded by a thick lymphocytic cuff [64]. The faith of the individual granuloma differs, with the more FDG-avid ones growing larger and acquiring central cavities while the less avid ones resolve [64]. The applications of FDG PET/CT in understanding the evolution of TB lesions have been translated to humans. In a recent study, Chen et al. showed the bronchi as the route of spread of infected caseum from cavitary lesions to uninvolved lung parenchyma leading to the formation of new areas of consolidation (figure 4) [67]. The bronchi connecting the cavity and new consolidation show increased FDG avidity, probably due to inflammation of the bronchial wall, their infected content, or a combination of both. The transbronchial pathway of spread was also used to show disease spread to the contralateral lung. Patients who developed new sites of disease involvement on a repeat FDG PET/CT obtained four weeks after the baseline scan were more likely to have two or more cavitary lesions in the lungs. This finding emphasizes the critical role these cavities play in disease spread to involved lung tissues and underscores the importance of the presence of cavity as a poor prognostic indicator in patients with PTB.

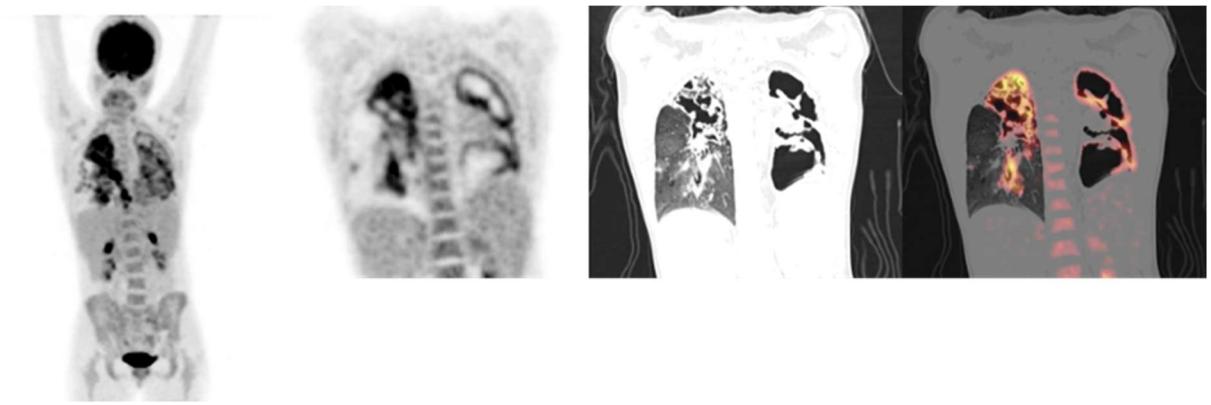

Figure 4: A 26-year-old female newly diagnosed with HIV infection. She was previously diagnosed with pulmonary tuberculosis and was commenced on anti-tuberculous treatment but defaulted. She represented with severe dyspnoea. FDG PET/CT images show multiple bilateral cavitary lesions. Re-evaluation confirmed infection with multi-drug resistant strain of *Mycobacterium tuberculosis*. Cavities in pulmonary tuberculosis portend poor prognosis as they are avenues for bacilli spread to uninvolved lung parenchyma, have high bacillary load, and have poor drug exposure.

A quarter of humanity harbor MTB in a latent infection with a 5-15% lifetime risk of reactivation [1,2]. The heterogeneity of latent TB infection (LTBI) is increasingly recognized [68]. It is imperative to develop biomarkers that identify patients at risk of reactivation and who may benefit from a full-course anti-tuberculous treatment versus patients with quiescent LTBI in whom chemoprophylaxis with a single agent may be sufficient for disease control. Lin et al. defined FDG PET/CT features that characterize LTBI with a greater potential for reactivation on immunosuppression in macaques [65]. Immunosuppression was induced in the experimental animals using TNF neutralization. Granulomas in the animals were classified as stable if SUV and size of granulomas remained stable following TNF neutralization or dynamic if SUV or size of granuloma increased (≥ 5units and ≥1mm, respectively). Among animals that reactivated after TNF neutralization, at least one dynamic granuloma was seen in 69% of them compared with 31% of animals without LTBI reactivation. On microbiological analysis, dynamic granulomas were more likely to contain bacilli compared with stable lesions. Reactivated animals were more likely to have more granulomas after TNF neutralization compared with non-reactivated animals. Animals who will experience LTBI reactivation had larger granulomas with higher FDG avidity compared with animals that did not. Similarly, the cumulative activity in FDG-avid mediastinal nodes was higher for animals that reactivated compared with animals that did not [65].

Esmail et al. have translated the application of FDG PET/CT for identifying LTBI with the potential to progress to active TB in a study involving 35 HIV-infected ART-naïve patients with LTBI based positive QuantiFERON Gold in-tube test (a test of prior exposure to TB antigen) [69]. All patients had a CD4 T-cell count of ≥350mm^{3,} consistent with the absence of severe immune dysfunction. Using FDG PET/CT, the authors identified a subset of 10 patients with FDG-avid lesions (lung infiltrates, fibrotic scars, and nodules) in the lungs, which they described as subclinical TB. The remaining 25 patients either had normal lung parenchyma (n=10) or discrete nodules (n=15). Four of the ten patients in the subclinical TB group developed active clinically overt TB within a median of 32 days after FDG PET/CT compared to no patient developing active TB in the 25 patients with LTBI. All patients with newly diagnosed HIV infection are screened for LTBI. Those with positive tests receive chemoprophylaxis with isoniazid [69]. This study demonstrates the potential of FDG PET/CT to identify the sub-group of patients among those with LTBI who have subclinical TB with a higher risk of progressing to active TB

and who may benefit from a full course of anti-tuberculous treatment rather than isoniazid monotherapy. Proactive treatment of subclinical TB may help in infection control as it may help prevent the subsequent development of open TB with sputum bacilli shedding.

3.3. FDG PET/CT for TB Treatment Response Assessment

The treatment of TB requires the administration of multiple drugs for a minimum of six months. Despite the development of multiple new effective anti-tuberculous drugs, efforts at shortening the duration of anti-tuberculous treatment (ATT) have remained unsuccessful as shorter regimens often lead to higher relapse rates [70]. A major factor responsible for the difficulty in developing shorter treatment courses is the limitations regarding the currently available response assessment tools. Early bactericidal activity (EBA) is a tool used in drug development. Unfortunately, drugs such as fluoroquinolones that have very high EBA in experimental animals have failed to produce non-inferior performance when used as part of drug combination for a shorter 4-month ATT course compared with the current standard of care of a 6-months course of ATT [71,72]. Clinically, sputum culture conversion at 2-month post ATT initiation is the most favored biomarker of treatment outcome and relapse prediction [73]. Two-month sputum conversion is a poor predictor of treatment outcome and relapse [74]. The pooled sensitivity and specificity of two-month sputum culture conversion for predicting relapse from a meta-analysis were 40% and 85%, respectively [75]. Another challenge with using sputum culture as a biomarker of response and relapse prediction is the time (a few weeks) required to obtain a positive culture. These clearly indicate a need for a better surrogate marker of treatment response and relapse prediction.

FDG PET/CT is a non-invasive biomarker for the real-time assessment of treatment response assessment in TB management. Due to the magnitude of the need for a biomarker with superior performance than the currently utilized markers of treatment response, the use of FDG PET/CT for the real-time assessment of bactericidal activity of anti-tuberculous drugs, prediction of treatment outcome, and the identification of patients at high risk of relapse are by far its most important indications in TB management. A head-to-head comparison of FDG PET/CT at two-month post ATT initiation performs better for response prediction than two-month sputum culture conversion [76]. This superior performance of FDG PET/CT during ATT relates to the decline in the intensity of radiotracer uptake in TB lesions with mycobacterial clearance. The change in the metabolic activity of the lesions as seen on FDG PET/CT occurs quite early and differs between treatment with a bactericidal regimen versus a bacteriostatic regimen, with the latter showing a slower rate of decline in lesions' metabolic activity [77]. Also, FDG PET/CT data can be used to show the superiority of drug combination over single-agent monotherapy [78]. The magnitude of response induced by a drug regimen in the nonhuman primate is similar to the response induced in humans by the same drug regimen [79], which indicates that all other factors being constant response data from animal studies can be extrapolated to humans. In a recent study, Xie et al. compared response assessment by EBA (daily bacterial count in expectorated sputum) versus FDG PET/CT data in 160 patients treated with different drug regimens of anti-tuberculous drugs, including monotherapies and drug combinations for 14 days [80]. Response data obtained from FDG PET/CT were more congruent with the clinical performance of agents tested than data from EBA. This supports the superiority of FDG PET/CT over the more laborious EBA for determining the early bactericidal activity of anti-tuberculous drugs. Based on the FDG PET/CT data, the authors identified the efficacy of individual drugs given as monotherapy and of multiple drugs given as combination therapies, identifying drug combinations that may be synergistic and those that may be antagonistic when combined for

treatment. Interestingly, the effectiveness of pyrazinamide was found to be associated with baseline inflammation, such that the more inflamed lesions respond better to pyrazinamide [80].

The increased susceptibility of people living with HIV to acquiring new and reactivating existing TB infections have been highlighted. Despite the current universal testing and treatment strategy in HIV management, some patients still present at advanced disease stage with severe immunosuppression. The institution of ART in these severely immunosuppressed patients often leads to the apparent worsening of existing opportunistic conditions and the appearance of new inflammatory/infectious conditions due to an exaggerated immune response to foreign and self-antigens, the so-called immune reconstitution and inflammatory syndrome (IRIS) [81,82]. The institution of ART in patients on ATT for TB may lead to the paradoxical worsening of disease symptoms and image findings [83]. FDG PET/CT obtained in these patients for interim response assessment during the process of IRIS may show worsening of disease (increased FDG avidity in lesions, new pulmonary and extrapulmonary lesions) [83,84]. This phenotype, which would hitherto be interpreted as disease progression/treatment failure, in the setting of IRIS, may be a sign of host immune response to MTB antigen. Patients at risk of TB IRIS often show higher baseline increased FDG avidity and volume of FDG-avid lesions compared with non-IRIS patients [84].

FDG PET/CT for treatment response assessment in EPTB

The role of FDG PET/CT for response assessment in EPTB may even be greater. While sputum culture conversion, despite its many limitations, is available for response assessment and relapse prediction in patients with PTB, tissue biopsy may be required to assess for sterilizing cure in EPTB. Tissue biopsy for the assessment of cure may be considered too invasive due to its associated risk as in EPTB involvement of the CNS. The duration for ATT is not as standardized for EPTB as it is for PTB. Though treatment for six months is recommended, patients often require ATT for longer to achieve a clinical cure. Some studies have evaluated the utility of FDG PET/CT for treatment response assessment in a mixed population of patients with EPTB involving different organs [85-89]. These studies, taken together, have provided some valuable insights. In patients who had FDG PET/CT for the initial assessment of PTB, a high SUVmax of the lung lesions is significantly associated with the presence of EPTB [87]. Following the institution of effective treatment, PET signals decline progressively [85-89]. New FDG-avid lesions may develop during treatment, possibly due to the progression of TB disease as in drug-resistant TB or FDG uptake in non-related conditions. Patients with this progression phenotype are at higher risk of unfavorable treatment outcomes, including death [85]. At treatment completion, only about of third of patients have normalization of FDG uptake at disease sites, while most patients considered cured according to the current standard of care still have significant residual FDG avidity in their lesions [89]. Some studies have evaluated the role of FDG PET/CT for treatment response assessment in specific subtypes of EPTB. Evidence on the utility of FDG PET/CT for treatment response assessment is available for only a few subtypes of EPTB and are considered below.

TB lymphadenitis: Lymph node involvement in TB is the commonest form of EPTB [36]. This is so, perhaps, because of the roles the lymph nodes play in the early stage of the disease [66]. Early works by Sathekge and colleagues demonstrated the utility of FDG PET/CT for assessing response to ATT in patients with tuberculous lymphadenitis [90,91]. These studies showed that higher SUVmax of involved lymph nodes, a higher number of lymph node basins involved, and a morphologic pattern of peripherally enhancing nodes with a hypoattenuating center were all significantly associated with poorer treatment outcomes (figure 5) [90,91]. The utility of FDG PET/CT for response assessment to ATT in TB lymphadenitis has also been described in a recent study reporting a durable cure in patients who achieved complete metabolic response to 6-month of ATT [92]. Again, patients

considered cured based on clinical parameters still had significant residual metabolic activity in the involved lymph nodes [92]. While some patients with residual metabolic activity on end-of-treatment FDG PET/CT had a durable cure, others were considered treatment failure based on the standard of care, and their treatment was consequently prolonged [93].

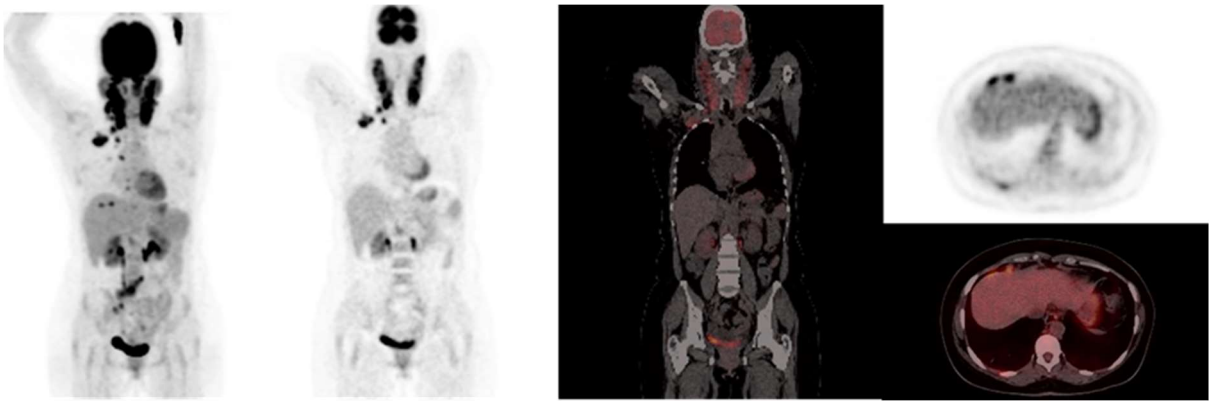

Figure 5: A 33-year-old female newly diagnosed with HIV infection (CD4+ T cell count = 12 cells/µL). Lymph node aspirate confirmed tuberculous lymphadenitis. FDG PET/CT showed widespread FDG-avid lymph nodes in multiple lymph node basins including bilateral cervical, mediastinal, mesenteric lymph node basins. There is involvement of the mesentery overlying the dome of the liver. These widespread nodal involvement with very intense FDG uptake suggest treatment-resistant phenotype.

Osteoarticular TB: The bones and joints are other common sites of EPTB involvement [36]. MTB spread to the spine is common via the hematogenous route (figure 6). TB spondylodiscitis is more likely to be associated with multi-level vertebral involvement and a higher SUVmax compared with pyogenic spondylodiscitis [57]. Also, there are often extra-spinal sites of disease involvement, especially in the lungs and lymph nodes in drainage zones beyond the lymph node draining basin of the involved vertebrae. These extra-spinal sites of disease involvement may serve as less invasive and suitable biopsy sites for the definitive diagnosis of EPTB [94,95]. Like findings in TB involvement of other organs, effective ATT is associated with a significant decline in FDG avidity of TB lesions in the spine, with FDG PET signal returning to normal with sterilizing cure [94,96]. Magnetic resonance imaging (MRI) is the gold-standard imaging modality for evaluating the spine. FDG PET/CT may, however, be more useful for TB spine response assessment as MRI may be contraindicated in specific categories of patients [97], including those with MRI-non-compatible metallic implants and claustrophobia. In a head-to-head comparison, FDG PET/CT outperformed spine MRI for treatment response assessment in patients with healed TB of the spine [97]. For peripheral bones, FDG PET/CT has a similarly good utility for response assessment, and patients who achieve complete metabolic response experience a durable cure [98].

Figure 6: A 44-year-old HIV-infected female (CD4+ T cell count=342 cells/µL). FDG PET/CT images show intense FDG uptake in multiple vertebrae and associated left psoas abscess. This was confirmed to be due to tuberculous spondylodiscitis. The risk of reactivation of latent infection and the acquisition of new disease among HIV-infected patients is not eliminated with immune recovery as seen in this patient with a relatively high CD4+ T cell count.

CNS TB: The CNS is a rare but important cause of morbidity and mortality among patients with EPTB. The brain is an obligate user of glucose for metabolism. Hence there is an intense physiologic uptake of FDG in the brain. Therefore, FDG PET/CT has traditionally been adjudged to be poorly sensitive for lesion detection in the brain. Recent studies have shown good lesion detection for FDG PET/CT in patients with CNS TB, with its sensitivity approaching that of MRI, the gold-standard imaging modality for the brain [99-101]. Whole-body imaging afforded by FDG PET/CT allows for the detection of extra-cranial sites of disease involvement, which can be quite common [102]. The encouraging lesion detection rate of FDG PET/CT for CNS TB should be an impetus to encourage a more rigorous evaluation of its role in treatment response assessment. For now, the evidence available is quite limited [36,102].

TB Pericarditis: MTB spread to the pericardium via direct spread from infected contiguous mediastinal lymph nodes or hematogeneously, with the hematogenous route commoner in people with HIV infection [103]. Imaging is often relied upon for diagnosing TB pericarditis due to the invasiveness of pericardial biopsy, and, more importantly, the high risk of sampling error during biopsy [104]. Interestingly, patients with low SUVmax of pericardial lesion on FDG PET/CT are more likely to have non-diagnostic pericardial biopsy results [104]. FDG uptake in the pericardium must be differentiated from other causes of pericarditis, including idiopathic (the most common form of pericarditis in the developed countries and often due to viral etiology), neoplastic, or due to pathogens other than MTB [103,104]. TB pericarditis is associated with the most intense pericardial FDG uptake compared with other causes of pericarditis [104]. TB pericarditis is more commonly associated with FDG-avid mediastinal and supraclavicular lymphadenopathy compared with idiopathic pericarditis [105]. These lymph nodes may be an easier target for biopsy for definitive EPTB diagnosis (figure 7). With successful treatment, FDG PET signals reduce considerably in the pericardium, making it a modality with potential utility for ATT response assessment [106,107].

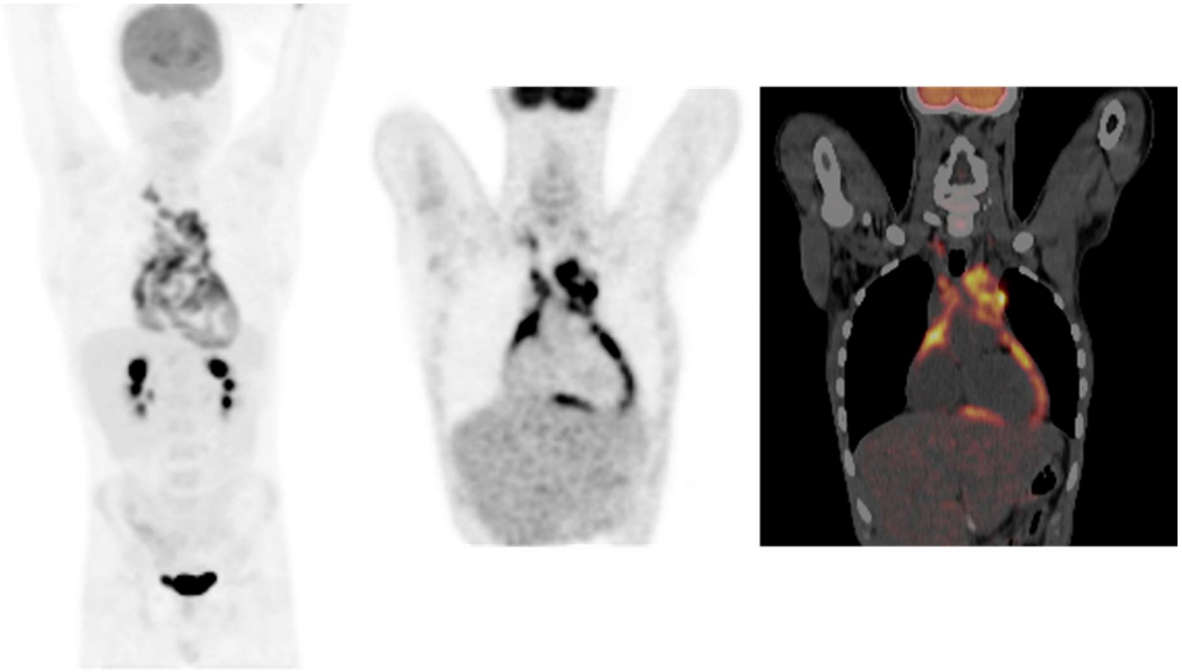

Figure 7: Tuberculous pericarditis. A 16-year-old male with an 11-year history of HIV infection with a sudden onset of chest pain. FDG PET/CT was obtained as part of his work-up. Images show intense FDG uptake in the pericardium and multiple mediastinal and right supraclavicular lymph nodes. The supraclavicular lymph node was biopsied and confirmed tuberculosis. Intense FDG uptake in the pericardium with associated mediastinal and/or supraclavicular lymphadenopathy are highly suggestive of tuberculosis. The involved lymph node can be biopsied for definitive diagnosis.

3.4. End-of-treatment FDG PET/CT for response assessment and relapse prediction

Useful information is derivable from the end-of-treatment (EOT) FDG PET/CT obtained after ATT is administered according to the current standard of care. Due to the heterogeneity of TB lesions in different patients, many patients who complete ATT for the recommended duration of treatment may have residual lesions on their EOT FDG PET/CT, which may be concerning for treatment failure. In this instance, treatment may be prolonged, especially when clinical evidence supports that therapy may have failed to produce a sterilizing cure. There are three possible scenarios on the EOT FDG PET/CT (figure 8). An assessment of complete metabolic response (CMR) to ATT is made when all lesions due to TB seen on baseline scan are no longer metabolically active on EOT FDG PET/CT, and there are no new lesions due to TB seen. CMR on EOT FDG PET/CT has an excellent correlation with sterilizing cure across several studies involving patients with PTB and EPTB [93,98,108]. On the other extreme is the progressive disease phenotype characterized by the persistence of all or some of the lesions seen on the baseline scan and the appearance of new lesions due to TB on the EOT FDG PET/CT. This pattern is not uncommon among patients who have completed ATT and are declared cured according to the standard of care based on the current clinical routine [109]. In the proper context, this pattern is suggestive of treatment failure. The persisting or residual metabolic pattern is between these extremes (CMR on one end and the progressive disease pattern on the other). In the residual metabolic pattern (RMA), some metabolic activity remains in the TB lesions on the EOT FDG PET/CT. RMA may be due to inflammation induced by persisting bacilli that have not been completely eradicated by ATT or antigen released by dead bacilli that continue to stimulate the host immune response.

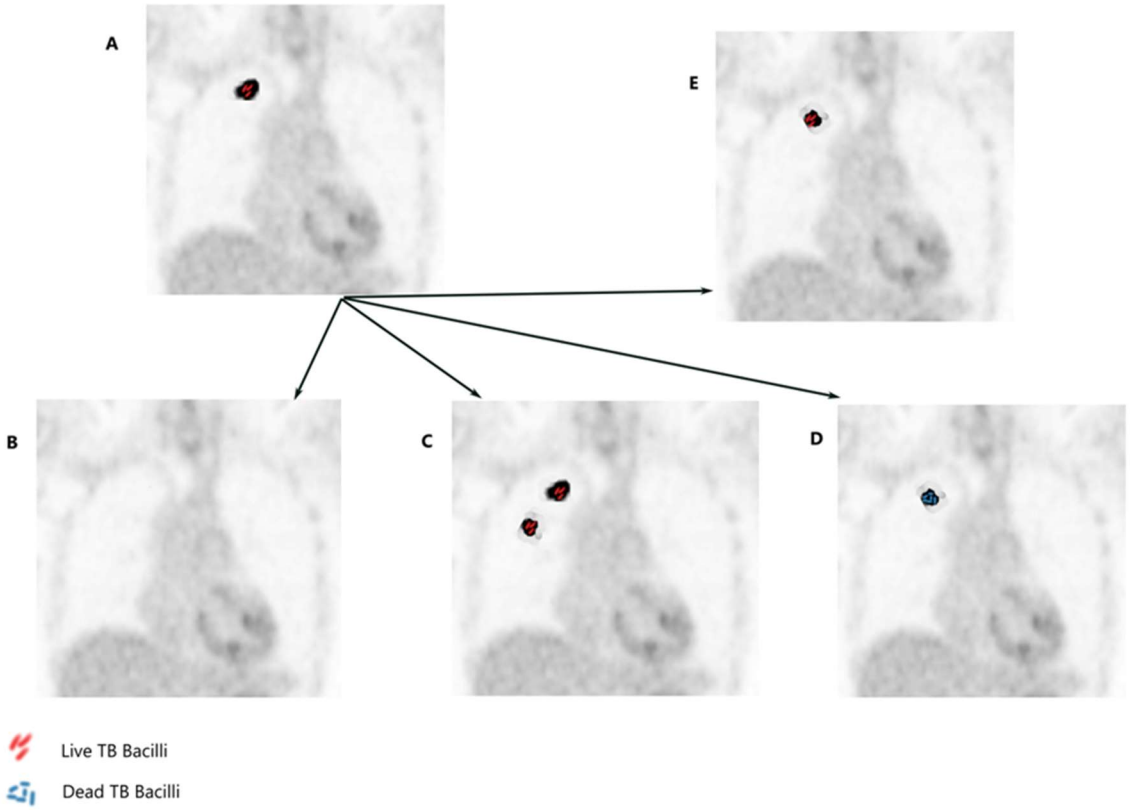

Figure 8: Figure: Images depicting the different uptake patterns on end-of-treatment FDG PET imaging. Baseline image (A) depict FDG-avid lesion in right upper lobe containing live bacilli. A complete metabolic response is shown in B, a finding predictive of a durable cure. Disease progression pattern is depicted in C with persistence of the lesion seen on the baseline scan and the appearance of another lesion, both of which contain live bacilli. This is consistent with treatment failure. Residual metabolic activity may be induced by antigenic stimulation by dead bacilli (D). On follow-up, this focus of residual metabolic activity resolves without further treatment, and it is not associated with a risk of relapse. Some patients may have residual metabolic activity that is induced by inactive or slowly replicating live bacilli (E). This pattern is associated with a risk of disease relapse due to the presence of these persisting live bacilli. At the present, it is not possible, based on FDG PET imaging findings only, to distinguish between pattern D without the risk of relapse and pattern E with associated risk of TB relapse.

Among the three phenotypes possible on EOT FDG PET/CT, the RMA pattern is the most common, seen in more than 50% of patients in most series [89,108,109]. RMA often co-exists with CT features of active TB in the lungs [110]. Their prevalence and the importance of differentiating RMA caused by live bacilli versus dead bacilli have made this pattern a subject of intense research in recent years [108-112]. Malherbe and colleagues isolated MTB mRNA from the sputum and bronchoalveolar lavage samples of patients declared cured based on the current standard of care but who had RMA on their EOT FDG PET/CT [109]. These results indicate the presence of replicating bacilli in the respiratory samples of these patients. Unlike DNA (which may be released following the disintegration of dead organisms), mRNA is only produced by replicating organisms. There are two sub-populations of MTB bacilli in TB disease, the actively replicating and the slowly replicating/inactive bacilli [113]. During treatment, the rapidly replicating bacilli are quickly eliminated while the slowly replicating/inactive bacilli are relatively resistant to elimination by TB chemotherapy agents [21]. These slowly replicating/inactive bacilli do not grow readily on culture

and may persist after successful treatment. They, therefore, represent an important cause of TB relapse in treated patients (figure 9). Described as differentially culturable MTB, these bacilli that do not grow on standard culture media were found to show positive culture when bronchoalveolar lavage samples (but not sputum samples) of patients with RMA on EOT FDG PET/CT were cultured using an enriched culture medium [111].

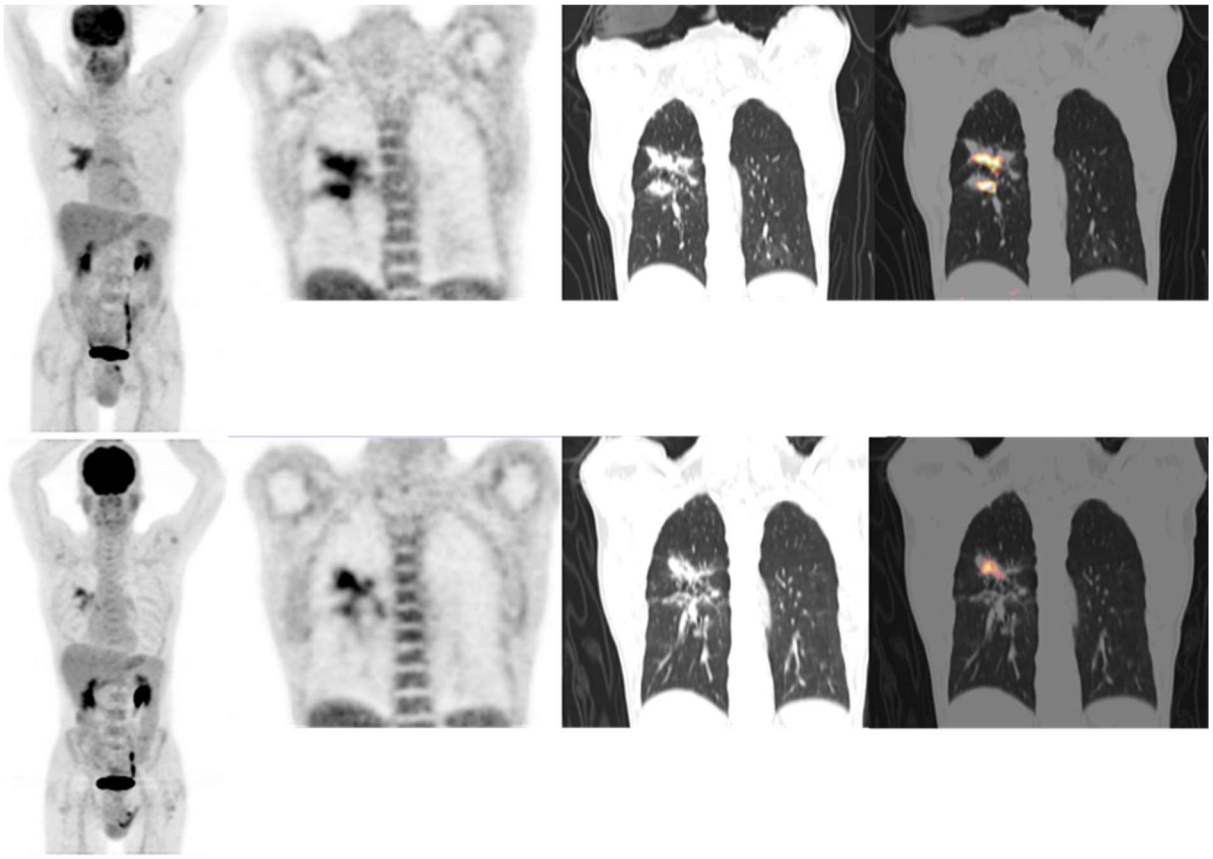

Figure 9: A 65-year-old male who completed a standard 6-month course of anti-tuberculous treatment. He was symptom-free and was gaining weight at the end of treatment. His sputum was negative for *Mycobacterium tuberculosis* growth. He was declared cured of tuberculosis based on these. An end-of treatment FDG PET/CT (top row) show two foci of increased FDG uptake in the right lung consistent with residual metabolic activity. Five months later, his respiratory symptoms recurred, and his sputum was positive for *Mycobacterium tuberculosis*, consistent with relapse of tuberculosis. Repeat FDG PET/CT (bottom row) show the persistence of the of the foci of increased FDG uptake in the right lung and an almost complete resolution of the other. No new lesion is seen. These findings suggest the presence of persisting bacilli at the end of treatment despite negative culture result.

4. Non-FDG Radiopharmaceuticals for PET Imaging of TB

FDG is, by far, the most utilized PET radiopharmaceutical for TB imaging in research and clinical practice. Other radiopharmaceuticals have been explored for TB imaging for several reasons. The most common reason for investigating the performance of non-FDG radiopharmaceuticals for PET imaging of TB is the search for an agent that will overcome the limitations of FDG, the most important being its lack of specificity for TB. FDG avidity of TB lesions is due to the radiopharmaceutical uptake by activated inflammatory cells that predominate in TB granulomas. FDG PET/CT, therefore, images the host immune response to MTB. Other radiopharmaceuticals targeting host immune response have been explored for PET imaging of TB [20]. There are other

metabolic processes that accompany inflammation within the TB granuloma, including hypoxia, angiogenesis, and fibrosis. Radiopharmaceuticals targeting these processes have been described in TB lesions.

4.1. Targeting iron utilization in TB

Iron is an essential micronutrient requirement by the host and MTB alike [114]. Macrophage is an important store of iron. A high macrophage iron store and nutritional iron overload enhance the susceptibility to acquiring TB disease and a severe disease phenotype [115]. To limit the iron available for microbial utilization, iron in the body is bound to proteins, including ferritin, lactoferrin, and transferrin [116]. Microbes obtain iron from these protein-bound iron by secreting siderophores [117]. Gallium is an iron-mimetic element that binds to transferrin following its intravenous administration. Increased vascular permeability at the site of infection increases the extravascular trafficking of the gallium-transferrin complex to the infection sites where the complex is phagocytosed by macrophages. Siderophores produced by the microbes are utilized to extract gallium from the gallium-transferrin complex in a manner analogous to iron extraction. Gallium-67, a SPECT tracer, is one of the earliest radionuclides used in TB imaging, exploring this essential requirement for iron in human TB infection [18,118,119]. The sub-optimal image quality of Gallium-67 scintigraphy, the high radiation burden it impacts on patients, the long duration of imaging (48 to 72 hours post tracer injection), and the introduction of FDG PET/CT to the clinics all contributed to the limited utilization of Gallium-67 scintigraphy for TB imaging.

Gallium-68 citrate (^{68}Ga citrate), a PET radiotracer, is now available and appears to address the limitations of Gallium-67 scintigraphy. An early study by Vorster et al. demonstrated the feasibility of ^{68}Ga-citrate PET/CT for imaging PTB and EPTB [120]. The study reported the superiority of ^{68}Ga-citrate PET/CT over stand-alone CT for TB lesion detection. In a subsequent work from the same group attempting to discriminate indeterminate lung lesions due to PTB versus other aetiologies, the level of ^{68}Ga-citrate uptake assessed by lesion SUVmax did not help make this differentiation [121]. In a head-to-head comparison of FDG PET/CT and ^{68}Ga-citrate PET/CT in patients with PTB and EBTB, FDG PET/CT showed better sensitivity than ^{68}Ga-citrate PET/CT for most sites of disease involvement except in the brain where ^{68}Ga-citrate PET/CT performed better in delineating brain parenchyma TB lesion than FDG PET/CT [122]. During ATT, the intensity of Ga-68 citrate uptake in TB lesions declined suggesting that ^{68}Ga-citrate PET/CT has the potential for use as a treatment response assessment tool. The lower sensitivity of ^{68}Ga-citrate PET/CT for TB lesion detection in most body regions is probably related to its lower signal-to-noise ratio compared with FDG PET/CT. Gallium-68 is highly protein-bound, which slows its trafficking to the tissue space, causing a high blood pool activity that contributes to the high background signal seen on ^{68}Ga-citrate PET/CT imaging acquired after the standard 60 minutes uptake period. This high blood pool activity limits lesion detection in the cardiovascular system and the identification of lymph nodes adjacent to major blood vessels [122].

4.2. Targeting host inflammatory response in TB with non-FDG PET radiopharmaceuticals

Several other molecular targets and metabolic pathways in activated inflammatory cells have been explored in PET imaging of TB. Such targets include somatostatin receptors and translocator protein. Metabolic pathways that are upregulated in infection, which have been targeted in PET TB imaging, including lipid, protein, and carbohydrate metabolisms. Like FDG, these radiopharmaceuticals targeting the host immune response to MTB lack specificity. Most importantly, none of them has consistently shown a superior performance than FDG in the characterization or treatment response assessment of TB. The most important advantage they bring to molecular imaging of TB is their lack of physiologic uptake in some organs, such as the brain and myocardium, with a known intense

accumulation of FDG. This makes these non-FDG radiopharmaceuticals suitable for assessing TB disease involvement in these organs.

^{68}Ga-DOTA-peptides target somatostatin receptors overexpressed by tumors arising from neural crest cells, especially well-differentiated neuroendocrine tumors [123,124]. Two studies have recently compared the performances of FDG PET and ^{68}Ga-DOTATOC PET among patients with TB [125,126]. The first studies compared the performances of FDG PET/MR and ^{68}Ga-DOTATOC PET/MR in a mixed group of patients with PTB, household contacts of patients with PTB, and patients with lobar pneumonia [125]. In the TB patients and the household contacts, FDG PET/MR detected more lesions and more intense radiotracer uptake in the lesions compared with ^{68}Ga-DOTATOC PET/MR. In the pneumonia group, both FDG and ^{68}Ga-DOTATOC showed significant tracer uptake in the lung lesion, with the former demonstrating more intense uptake in the lesions than the latter. The results from the second study are largely similar, with the authors reporting generally higher SUVmax for pulmonary lesions and mediastinal lymph nodes on the FDG PET/CT compared with ^{68}Ga-DOTATOC PET/CT [126]. Put together, these two small studies show that the signal-to-noise ratio is much better on FDG PET compared with ^{68}Ga-DOTATOC PET in lung and lymph node disease due to TB, a finding that may account for the superior diagnostic sensitivity of the former compared with the latter. The theoretical advantage of targeting somatostatin receptor expression in activated macrophages in TB granuloma will be in assessing EPTB of the CNS and pericardium, two important forms of EPTB in which the physiologic uptake of FDG may mask lesion detection in the involved organs. This potential indication remains to be explored.

^{11}C-methionine is a radiolabelled amino acid that has been used as a biomarker for evaluating amino acid utilization in tumors and inflammatory cells. In a head-to-head comparison of ^{11}C-methionine PET/CT and FDG PET/CT in patients with intracranial TB, both scans detected the brain TB lesions in all treatment-naïve patients and a single patient that had been on ATT for eight weeks prior to the scans [127]. ^{11}C-methionine PET, however, showed better lesion contrast than FDG PET due to the absence of physiologic ^{11}C-methionine uptake in the brain. These results are preliminary, and more works are needed to define the role of ^{11}C-methionine PET/CT in the molecular imaging of TB.

^{18}F-fluoroacetate, a radiotracer that targets fatty acid metabolism that is upregulated in tumor and inflammatory cells, has also been explored for imaging TB and other infectious diseases [128]. The common denominator to all these radiopharmaceuticals targeting host immune inflammatory response is their lack of specificity. Pathogen-specific imaging holds promise to address this limitation. Trehalose is a non-mammalian disaccharide that is essential for the synthesis of the unique mycobacterial cell wall. The results of a preliminary in vitro investigation of radiolabelled trehalose as a potential radiotracer for TB imaging has been reported [129,130]. More work and eventual clinical translation of this agent are anticipated for the future.

Neutrophils are among the cellular constituents of TB granuloma. Their role in the evolution and severity of TB infection is still being evaluated. Available evidence suggests neutrophils produce pro- and anti-inflammatory cytokines [131]. Neutrophils phagocytosed MTB but are ineffective in orchestrating their intracellular destruction. The motility of neutrophils from granuloma to other body parts suggests they may play a role in MTB dissemination to distant sites [132]. Molecular imaging offers the potential for the non-invasive interrogation of biological processes [133]. It, therefore, holds promise to study the impact of neutrophil invasion of TB granuloma and its trafficking [134]. Two tracers have been investigated for their ability to target specific subpopulations of immune cells in TB granuloma. [^{64}Cu]-LLP2A is a PET probe that targets very late antigen-4 (VLA-4), an integrin expressed by inflammatory cells. In a preclinical study, [^{64}Cu]-LLP2A was shown to target macrophages, T cells, and to a lesser extent, neutrophils in TB granuloma [135].

^{64}Cu-FLFLF, a PET probe for formyl peptide receptor 1 (FPRI), was subsequently investigated for its ability to specifically target neutrophils within TB granuloma. In a macaque model of TB granuloma, ^{64}Cu-FLFLF binds to neutrophils within granulomas but with significant binding to macrophages as well [136]. While the search for a probe that specifically targets neutrophils continues, an important insight from this study is the potential of molecular imaging to study the temporal changes in cellular composition and metabolism of TB granuloma [135,137].

4.3. Targeting Hypoxia in TB

The lesions induced by TB in the lungs of humans and non-human primates are varied, including lung consolidation, nodules and micronodules, fibrocystic changes, and cavitary lesions. The biology of the bacilli that populate these different lesions also differs. For example, lung cavities in PTB are well-aerated as they are often in direct communication with the airway. The walls of the cavities thus have a large population of bacilli, which are actively replicating and are most susceptible to acquiring new mutations that confer drug resistance [138]. Long-standing granulomas with thick surrounding fibrotic cuff and central caseous necrosis are very hypoxic and contain fewer slowly or dormant bacilli [139,140]. These slowly replicating or dormant bacilli are relative resistance to ATT and may contribute to the persisting FDG signal seen on EOT FDG PET/CT [141]. Studying hypoxia, therefore, offers an avenue to understanding one of the major drivers of treatment failure.

Fluorine-18 fluoromisonidazole ([^{18}F]FMISO), a fluorinated nitroimidazole compound, is trapped in hypoxic but not normoxic tissues. Belton et al. demonstrated the presence of hypoxia in patients with PTB using [^{18}F]FMISO PET/CT [142]. The popularity of ^{68}Germanium/^{68}Gallium generator in many nuclear medicine facilities providing a year-round supply of radio-gallium and the advances in the click chemistry of ^{68}Ga allowing it to be complexed to various biological molecules have popularized ^{68}Ga-labelled radiopharmaceuticals for PET/CT imaging of many biological processes seen in inflammation, infection, and oncologic conditions. Consequently, there has been a recent interest in developing ^{68}Ga-labelled PET radiopharmaceuticals for hypoxic imaging in oncology and infection [143,144]. ^{68}Ga-nitroimidazole uptake quantified as hypoxic tumor volume on PET imaging has been reported to correlate with the tumor expression of hypoxia-inducible factor-1α (HIF-1α) in patients with carcinoma of the cervix uteri [145]. More recently, the potential of ^{68}Ga-nitroimidazole for hypoxia imaging in TB patients has been reported [146]. There was ^{68}Ga-nitroimidazole uptake in TB lesions above background activity with varying levels of radiotracer uptake in different TB lesions. These preliminary works establishing the feasibility of the use of PET probes for the non-invasive imaging of hypoxia in TB hold much potential for future applications in understanding the level of hypoxia in different types of lesions, the temporal changes in lesion hypoxia during the evolution of the disease, and the impact of hypoxia on lesion response to chemotherapy during ATT.

4.4. Targeting angiogenesis in TB

TB-infected macrophages secrete vascular endothelial growth factor (VEGF), inducing the formation of new blood vessels [147]. These new blood vessels promote hematogenous bacilli dissemination to distant sites, contributing to pathogen virulence [147]. ^{68}Ga-Alfatide II is a PET radiopharmaceutical that targets $\alpha_v\beta_3$ integrin expressed on neovasculature. The intensity of ^{68}Ga-Alfatide II as a marker of angiogenesis has been compared in TB versus non-small cell lung cancer (NSCLC) patients [148]. The mean SUVmax of ^{68}Ga-Alfatide II uptake in NSCLC was 3.83 ± 0.22 compared with 2.29 ± 0.20 for TB lesions. These results, which others have replicated, suggest the presence of angiogenesis in NSCLC and TB, though the higher level of uptake in NSCLC suggests a higher level of angiogenesis in malignancy (NSCLC) compared with TB [148,149].

Prostate-specific membrane antigen (PSMA) is a target overexpressed in metastatic prostate cancer. PSMA is not prostate-specific and has been reported in the neovasculature of several malignant and benign conditions seen as ^{68}Ga-PSMA uptake in these lesions on PET/CT images [150]. Pyka and colleagues reported the uptake of ^{68}Ga-PSMA in the PTB lesions [151]. Incidental uptake of ^{68}Ga-PSMA on PET/CT imaging in pulmonary and extrapulmonary sites has been reported by others as well [152-155]. The important takeaway from these reports of ^{68}Ga-PSMA uptake in TB lesions is for readers to be aware of TB as a possible cause of abnormal radiotracer uptake on ^{68}Ga PSMA PET/CT scan and to consider this as a differential diagnosis in the suggestive setting (figure 10).

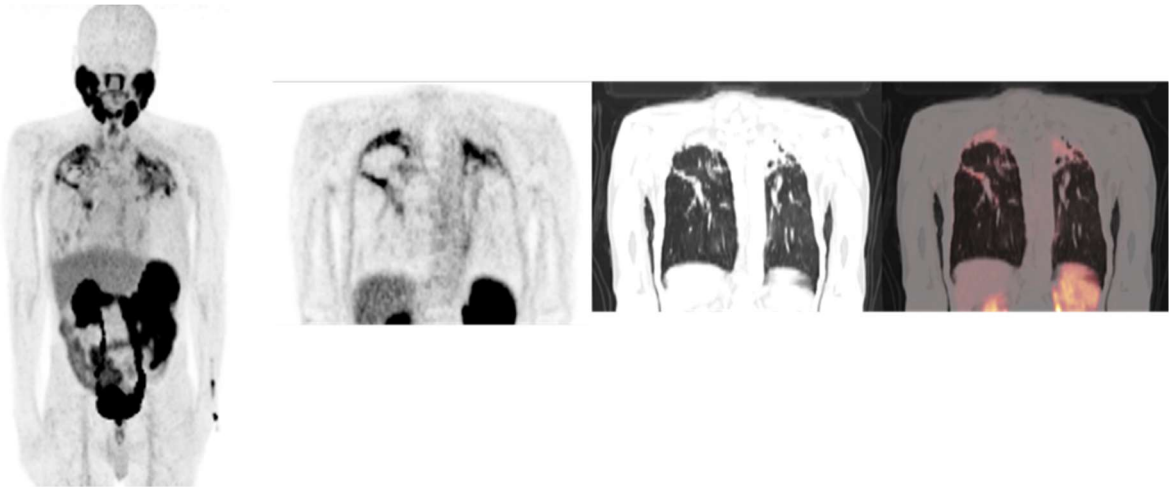

Figure 10: A 69-year-old male with newly diagnosed adenocarcinoma of the prostate gland. ^{68}Ga-PSMA PET/CT was obtained for the initial staging of his disease. No evidence of prostate cancer metastasis is seen. Bilateral radiotracer-avid upper lobe fibrocystic lung changes are seen. On further questioning, the patient gave a history of ongoing ant-tuberculous treatment for pulmonary tuberculosis. Tuberculosis is ^{68}Ga-PSMA-avid due to PSMA expression in tuberculoma associated neovasculature. This must be borne in mind when interpreting radiotracer-avid lung lesions on ^{68}Ga-PSMA PET/CT scans.

4.5. Targeting fibrosis in TB

A key feature of TB granuloma is the formation of a dense fibrotic cuff around the focus of infection [156]. PET probes targeting fibrosis can, therefore, demonstrate tracer retention on imaging in fibrotic TB lesions. Fibroblast activation protein (FAP) is a molecular target expressed by activated fibroblasts associated with benign and malignant conditions. Radiolabelled inhibitors of FAP (^{68}Ga-FAPI) have been synthesized for PET imaging of different malignant conditions [157-159]. Several cases of incidental ^{68}Ga-FAPI uptake in PTB and EPTB have been reported, mostly in patients imaged for other indications [160,161]. Like with ^{68}Ga-PSMA, these reports should raise awareness regarding TB as a possible pitfall that should be borne in mind when interpreting ^{68}Ga-FAPI PET/CT imaging acquired for other indications.

5. Molecular Imaging with Radiolabelled Anti-tuberculous Drugs for Pharmacokinetic Studies

The optimum drug concentration at the infection site is a prerequisite for effective microbial killing [162]. Sub-optimal exposure of MTB to chemotherapy agents is an important cause of treatment failure and the development of drug resistance [163]. In the preclinical phase of drug development, the pharmacokinetic data of the experimental drug are obtained from animal studies. These data are extrapolated for the initial human studies. In humans, drug kinetics data are obtained from repeated plasma sampling. Plasma drug concentrations do not always reflect concentration in different tissue

spaces [162]. The heterogeneity of TB lesions regarding their structural composition, vascularity, and bacillary load may be an additional factor making extrapolation of intralesional drug concentrations from plasm drug concentration less reliable [164]. The actual determination of drug concentration in TB lesions requires the surgical resection of the lesions, which is done in only a few cases of clinical TB. The radiolabelling of anti-tuberculous drugs with positron-emitting radionuclide and the study of their in vivo kinetics in experimental animals and humans using PET have been described. Anti-tuberculous drugs that have been successfully radiolabeled with positron-emitting radionuclide for PET imaging include the first-line agents such as rifampicin [165], isoniazid [166], and pyrazinamide [167]. The newer anti-tuberculosis drugs such as bedaquiline and linezolid, commonly used as second-line agents in multi-drug resistance TB, have also been radiolabeled, and their biokinetics studied using PET [168,169].

PET for pharmacokinetic studies of drugs offers several advantages over the traditional methods. PET offers a non-invasive avenue to study drug concentration in different tissue compartments without perturbing the internal milieu or sacrificing the animals, offering a cost-effective method for pharmacokinetic studies. Repeated evaluation is possible with PET, which allows for studying the temporal changes in drug kinetics during disease evolution and treatment [164].

Important insights have been derived from studies evaluating the pharmacokinetics of rifampicin in experimental animals and humans [165,170-172]. In an animal model of PTB, necrotic TB lesions had significantly lower drug exposures compared with normal lung tissues [165]. The cavity has the largest bacilli burden among the different types of lung lesions induced by MTB [138,170]. Despite this, cavities showed the lowest drug exposure compared with other types of TB lesions [170]. This finding has significant implications for drug effectiveness and drug resistance development. The exploration of the strength of PET imaging as a tool for studying the temporal kinetics of drugs during treatment has shown that while plasma concentration of rifampicin remains stable, drug exposure of cavitary TB lesions reduces over time [170]. These pharmacokinetic insights provided by PET may contribute to the worse prognosis seen in cavitary PTB. Tuberculous meningitis is the most devasting form of TB due to the high morbidity and mortality associated with it. PET-based pharmacokinetics has shown a limitation in the penetration of rifampicin into the brain affected by tuberculous meningitis, with the level of penetration decreasing substantially from the second week of treatment [172]. The penetration of rifampicin into the brain parenchyma and brain lesions is driven by the disruption in the blood-brain barrier brought about by tuberculous meningitis [171]. The improvement in blood-brain barrier integrity with treatment accounts for the progressive decline in the rate of drug penetration into the brain. PET-derived data also showed that increasing the dose of rifampicin administered for treatment may help attain the optimum intralesional drug concentration [172]. Also, there were no correlations between rifampicin concentration in the cerebrospinal fluid (CSF) and brain lesions [172], underscoring the non-reliability of CSF sampling for predicting intralesional drug exposure and the need for a non-invasive tool for more accurate measurement of drug concentrations at the actual disease sites.

Isoniazid is another first-line anti-tuberculous agent which has been successfully radiolabelled and used to model the in vivo kinetics of the drug [166]. In addition to modeling the in vivo biokinetics of isoniazid, radiolabeled-isoniazid can be used as a probe for pathogens-specific imaging due to its ability to accumulate within the tubercle bacilli. For its intracellular trapping within the bacilli, isoniazid is transformed into its active metabolite using mycobacterial enzymes. Mutation in KatG, the gene that codes for the activating mycobacterial enzymes, is one of the most important modes of isoniazid resistance by MTB. Radiolabelled isoniazid, therefore, has the potential for use as a non-invasive probe to interrogate infection by resistant strains of MTB.

6. Conclusion and Future Perspectives

Molecular imaging using PET has evolved to become a useful tool with several applications in the clinical management and research of TB. Its importance and applications are increasing due to the limitations in the performance of the currently applied tools for TB diagnosis, treatment response assessment, and relapse prediction. Despite being one of the oldest infection diseases known to man, much remains to be known about the drivers of the heterogeneity in the disease course and the lesions induced by MTB, hence, TB continues to be a major cause of death from an infectious agent. FDG has become the most utilized radiopharmaceutical for PET imaging of TB. The most important clinical use of FDG PET/CT in TB management appears to be in treatment response assessment, where it has been shown to identify sterilizing cure with a high consistency across studies. When applied at the end of treatment, FDG PET/CT can identify a group of patients who, despite being declared cured based on the current standard of cure, still harbors live bacilli capable of causing disease relapse. A need exists for a correlative marker to differentiate this group of patients with RMA on their EOT FDG PET with persisting bacilli who are at risk of TB relapse versus patients with RMA induced by antigen shed by dead bacilli but have achieved sterilizing cure without the risk of relapse. When used for the initial assessment of disease or as a complementary tool for TB diagnosis, FDG PET/CT helps determine the whole-body burden of disease, predict treatment outcomes, and probably guide management. Our understanding of the pathogenesis and the evolution of the lesions induced by MTB is improving through the application of FDG PET/CT as a non-invasive biomarker to understudy these aspects of the disease. FDG is a non-specific marker of host inflammatory response to MTB, an important limitation to its use. Efforts are in progress to develop other radiopharmaceuticals without this limitation of FDG for PET imaging of TB.

Successful radiolabelling of anti-tuberculous drugs for PET imaging of their in vivo biodistribution has opened another opportunity to apply molecular imaging in TB. With this technique, it is now possible to determine the drug exposure of different TB lesions, compare drug levels in different body compartments, and track the spatial and temporal differences in drug exposures of different lesions during TB treatment. The new total-body PET camera offers a unique opportunity to perform dynamic imaging to determine the in vivo biokinetics of drugs in different tissues compartment and different lesions anywhere in the body with a single bed position after an intravenous administration of a radiolabeled anti-tuberculous agent of choice.

Molecular imaging in TB is highly under-utilized in clinical and research applications. The under-utilization of molecular imaging techniques in the clinical management of TB, especially with PET, is most likely related to cost and availability. PET is a relatively expensive technique. Facilities offering PET are limited to large urban centers in most developing countries where TB cases are most prevalent. These factors combine to make the use of molecular imaging techniques in the routine management of TB not feasible at the current time. Concerted efforts toward conducting large-scale multicentre studies are required to better define the indications for which PET imaging may be most suitable and the categories of patients in whom it would make a meaningful impact on their treatment outcome. Molecular imaging with PET is still highly underutilized in TB research despite the many opportunities it offers for cost-effective investigation of the different aspects of TB infection and disease. The utilization of the PET technique in TB research is currently limited to a few groups in the United States and South Africa and their collaborators in a few other countries. Therefore, more awareness is needed to broaden the application of molecular imaging techniques in TB research.

References

1. Houben RM, Dodd PJ: The global burden of latent tuberculosis infection: a re-estimation using mathematical modelling. PLoS Med 13:e1002152, 2016
2. Vynnycky E, Fine PE: Lifetime risks, incubation period, and serial interval of tuberculosis. Am J Epidemiol 152:247-263, 2000
3. Glaziou P, Floyd K, Raviglione MC: Global Epidemiology of Tuberculosis. Semin Respir Crit Care Med 39:271-285, 2018
4. Marais BJ, Lönnroth K, Lawn SD et al: Tuberculosis comorbidity with communicable and non-communicable diseases: integrating health services and control efforts. Lancet Infect Dis 13:436-448, 2013
5. Lönnroth K, Jaramillo E, William BC, et al: Drivers of tuberculosis epidemics: the role of risk factors and social determinants. Soc Sci Med 68:2240-2246, 2009
6. Pranveer S, Kumar SV, Ramsevak K: Diagnosis of TB: From conventional to modern molecular protocols. Front Biosci (Elite Ed) 11:38-60, 2019
7. Van der Kuyp F, Mahan CS: Prolonged positivity of sputum smears with negative cultures during treatment for pulmonary tuberculosis. Int J Tuberc Lung Dis 2012:1663-1667, 2012
8. Phillips PPJ, Mendel CM, Nunn AJ, et al: A comparison of liquid and solid culture for determining relapse and durable cure in phase III TB trials for new regimens. BMC Med 15:207, 2017
9. Zifodya JS, Kreniske JS, Schiller I, et al: Xpert Ultra versus Xpert MTB/RIF for pulmonary tuberculosis and rifampicin resistance in adults with presumptive pulmonary tuberculosis. Cochrane Database Syst Rev 2:CD009593, 2021
10. Gati S, Chetty R, Wilson D, et al: Utilization and Clinical value of Diagnostic Modalities for Tuberculosis in a High HIV Prevalence Setting. Am J Trop Med Hyg 99:317-322, 2018
11. Cudahy PGT, Dawson R, Allwood BW, et al: Diagnostic outcomes after chest radiograph interpretation in patients with suspected tuberculosis and negative sputum smears in a high-burden human immunodeficiency virus and tuberculosis setting. Open Forum Infect Dis 4:ofx123, 2017
12. Nakiyingi L, Bwanika JM, Ssengooba W, et al: Chest X-ray interpretation does not complement Xpert MTB/RIF in diagnosis of smear-negative pulmonary tuberculosis among TB-HIV co-infected adults in a resource-limited setting. BMC Infect Dis 21:63, 2021
13. Ko JM, Park HJ, Kim CH, et al: The relation between CT findings and sputum microbiology studies in active pulmonary tuberculosis. Eur J Radiol 84:2339-2344, 2015
14. Ors F, Deniz O, Bozlar U, et al: High-resolution CT findings in patients with pulmonary tuberculosis: correlation with the degree of smear positivity. J Thorac Imaging 22:154-159, 2007
15. Siemsen JK, Grebe SF, Sargent EN, et al: Gallium-67 scintigraphy of pulmonary diseases as a complement to radiology. Radiology 118:371-375, 1976
16. Palestro CJ, Goldsmith SJ: The role of gallium and labelled leukocyte scintigraphy in the AIDS patients. Q J Nucl Med 39:221-230, 1995
17. Goldfarb CR, Colp C, Ongseng F, et al: Gallium scanning in the 'new' tuberculosis. Clin Nucl Med 22:470-474, 1997
18. Schuster DM, Alazraki N: Gallium and Other Agents in Diseases of the Lung. Semin Nucl Med 32:193-211, 2002
19. Yeh JJ, Huang YC, Teng WB, et al: The role of gallium-67 scintigraphy in comparing inflammatory activity between tuberculous and nontuberculous mycobacterial pulmonary disease. Nucl Med Commun 32:392-401, 2011

20. Ankrah AO, Glaudemans AWJM, Maes A, et al: Tuberculosis. Semin Nucl Med 48:108-130, 2018
21. Sathekge MM, Ankrah AO, Lawal I, et al: Monitoring response to therapy. Semin Nucl Med 48:166-181, 2018
22. Philips JA, Ernst JD: Tuberculosis pathogenesis and immunity. Annu Rev Pathol 7:353-84, 2012
23. Serbina NV, Flynn JL: CD8(+) T cells participate in the memory immune response to Mycobacterium tuberculosis. Infect Immun 69:4320-4328, 2021
24. Ghanavi J, Farnia P, Farnia P, et al: The role of interferon-gamma and interferon-gamma receptor in tuberculosis and nontuberculous mycobacterial infections. Int J Mycobacteriol 10:349-357, 2021
25. McAdam AJ, Milner DA, Sharpe AH: Infectious Diseases, in Kumar V, Abbas AK, Aster JC (eds): Robbins and Cotran Pathologic Basis of Disease (ed 9). Philadelphia, PA, Saunders, 2015
26. Ehlers S, Schaible UE: The granuloma in tuberculosis: dynamics of a host-pathogen collusion. Front Immunol 3:411, 2013
27. Flynn JL, Goldstein MM, Chan J, et al: Tumor necrosis factor-alpha is required in the protective immune response against Mycobacterium tuberculosis in mice. Immunity 2:561-572, 1995
28. Gideon HP, Phuah J, Myers AJ, et al: Variability in tuberculosis granuloma T cell responses exists, but a balance of pro- and anti-inflammatory cytokines is associated with sterilization. PLoS Pathog 11:e1004603, 2015
29. Lawal I, Zeevaart J, Ebenhan T, et al: Metabolic Imaging of Infection. J Nucl Med 58:1727-1732, 2017
30. Lawal IO, Mokoala KMG, Kgatle MM, et al: Radionuclide Imaging of Invasive Fungal Disease in Immunocompromised Hosts. Diagnostics (Basel) 11:2057, 2021
31. Ankrah AO, van der Werf TS, de Vries EF, et al: PET/CT imaging of *Mycobacterium tuberculosis* infection. Clin Transl Imaging 4:131-144, 2016
32. Skoura E, Zumla A, Bomanji J: Imaging in tuberculosis. Int J Infect Dis 32:87-93, 2015
33. Soussan M, Brillet PY, Mekinian A, et al: Patterns of pulmonary tuberculosis on FDG-PET/CT. Eur J Radiol 81:2872-2876, 2012
34. Urs VL, Rizvi I, Kumar N, et al: Concurrent central nervous system involvement in immunocompetent adults with pulmonary miliary TB: a prospective analysis. Trans R Soc Trop Med Hyg 116:344-351, 2022
35. Philip N, William T, John DV: Diagnosis of tuberculous meningitis: challenges and promises. Malays J Pathol 37:1-9, 2015
36. Bomanji J, Sharma R, Mittal BR, et al: PET/CT features of extrapulmonary tuberculosis at first clinical presentation: a cross-sectional observational ^{18}F-FDG imaging study across six countries. Eur Respir J 55:1901959, 2020
37. Wright WF, Yenokyan G, Simmer PJ, et al: Geographical variation of infectious disease diagnoses among patients with fever of unknown origin: A systematic review and meta-analysis. Open Forum Infect Dis. 9:0fac151, 2022
38. Keidar Z, Gurman-Balbir A, Gaitini D, et al: Fever of unknown origin: The role of ^{18}F-FDG PET/CT. J Nucl Med 49:1980-1985, 2008
39. Wang Q, Li YM, Li Y, et al: 18F-FDG PET/CT in fever of unknown origin and inflammation of unknown origin: a Chinese multi-centre study. Eur J Nucl Med Mol Imaging 46:159-165, 2019
40. Kouijzer IJE, Mulders-Manders CM, Bleeker-Rovers CP, et al: Fever of unknown origin: the value of FDG-PET/CT. Semin Nucl Med 48:100-107, 2018

41. Bruchfeld J, Correia-Neves M, Källenius G: Tuberculosis and HIV coinfection. Cold Spring Herb Perspect Med 5:a017871, 2015
42. Lodi S, del Amo J, d'Arminio Monforte A, et al: Risk of tuberculosis following HIV seroconversion in high-income countries. Thorax 68:207-213, 2013
43. Castaigne C, Tondeur M, de Wit S, et al: Clinical value of FDG-PET/CT for the diagnosis of human immunodeficiency virus-associated fever of unknown origin: a retrospective study. Nucl Med Commun 30:41-47, 2009
44. Martin C, Castaigne C, Tondeur M, et al: Role of interpretation of fluorodeoxyglucose-positron emission tomography/computed tomography in HIV-infected patients with fever of unknown origin: a prospective study. HIV Med 14:455-462, 2013
45. Okada RC, Barry PM, Skarbinski J, et al: Epidemiology, detection, and management of tuberculosis among end-stage renal disease patients. Infect Control Hosp Epidemiol 39:1367-1374, 2018
46. Fang HC, Lee PT, Chen CL, et al: Tuberculosis in patients with end-stage renal disease. Int J Tuberc Lung Dis 8:92-97, 2004
47. Tek Chand K, Chennu KK, Amancharla Y, et al: Utility of 18F-FDG PET/CT scan to diagnose the etiology of fever of unknown origin in patients on dialysis. Hemodial Int 21:224-231, 2017
48. Lawal IO, Popoola GO, Lengana T, et al: Diagnostic utility of ^{18}F-FDG PET/CT in fever of unknown origin among patients with end-stage renal disease treated with renal replacement therapy. Hell J Nucl Med 22:70-75, 2019
49. Sathekge MM, Maes A, Pottel H, et al: Dual time-point FDG PET-CT for differentiating benign from malignant solitary pulmonary nodules in a TB endemic area. S Afr Med J 100:598-601, 2010
50. Chen S, Li X, Chen M, et al: Limited diagnostic value of Dual-Time-Point (18)F-FDG PET/CT imaging for classifying solitary pulmonary nodules in granuloma-endemic regions both at visual and quantitative analyses. Eur J Radiol 85:1744-1749, 2016
51. Lococo F, Muoio B, Chiappetta M, et al: Diagnostic performance of PET or PET/CT with different radiotracers in patients with suspicious lung cancer or pleural tumors according to published meta-analyses. Contrast Media Mol Imaging 2020:5282698, 2020
52. Tsao CH, Wu CY, Chang CW, et al: Micro-PET imaging of [^{18}F]fluoroacetate combined with [^{18}F]FDG to differentiate chronic *Mycobacterial tuberculosis* infection from an acute bacterial infection in a mouse model: a preliminary study. Nucl Med Commun 40:639-644, 2019
53. Del Giudice, Bianco A, Cennamo A, et al: Lung and nodal involvement in nontuberculous Mycobacterial disease: PET/CT role. Biomed Res Int 2015:353202, 2015
54. Özmen Ö, Tatci E, Demiröz M, et al: Is 18F-FDG PET/CT capable of differential diagnosis from tuberculous pleurisy from malignant mesothelioma? Nucl Med Commun 42:672-677, 2021
55. Duan H, Xu D, Lu R, et al: Characterizing omental PET/CT findings for differentiating tuberculous peritonitis from peritoneal carcinomatosis. Abdom Radiol 46:5574-5585, 2021
56. Wang SB, He W, Xv DD, et al: Visual PET/CT scoring of mesenteric FDG uptake to differentiate between tuberculous peritonitis and peritoneal carcinomatosis. Diagn Interv Radiol 26:523-530, 2020
57. Bassetti M, Merelli M, Di Gregorio F, et al: Higher fluorine-18 fluorodeoxyglucose positron emission tomography (FDG-PET) uptake in tuberculous compared to bacterial spondylodiscitis. Skeletal Radiol 46:777-783, 2017
58. Gunes BY, Onsel C, Sonmezoglu K, et al: Diagnostic value of F-18 FDG PET/CT in patients with spondylodiscitis: Is dual time point imaging time worthy? Diag Microbiol Infect Dis 85:381-385, 2016

59. Basaraba RJ: Experimental tuberculosis: the role of comparative pathology in the discovery of improved tuberculosis treatment strategies. Tuberculosis (Edinb) 88 (suppl 1):S35-S47, 2008
60. Williams CM, Abdulwhhab M, Birring SS, et al: Exhaled *Mycobacterium tuberculosis* output and detection of subclinical disease by face-mask sampling: prospective observational studies. Lancet Infect Dis 20:607-617, 2020
61. Coleman MT, Maiello P, Tomko J, et al: Early Changes by ^{18}Fluorodeoxyglucose Positron Emission Tomography Coregistered with Computed Tomography Predict Outcome after *Mycobacterium tuberculosis* Infection in Cynomolgus Macaques. Infect Immun 82:2400-2404, 2014
62. Gregg RW, Maiello P, Borish HJ, et al: Spatial and temporal evolution of lung granulomas in a cynomolgus macaque model of *Mycobacterium tuberculosis* infection. Radiol Infect Dis 5:110-117, 2018
63. White AG, Maiello P, Coleman MT, et al: Analysis of ^{18}FDG PET/CT Imaging as a Tool for Studying *Mycobacterium tuberculosis* Infection and Treatment in Non-human Primates. J Vis Exp 127:e56375, 2017
64. Via LE, Schimel D, Weiner DM, et al: Infection Dynamics and Response to Chemotherapy in a Rabbit Model of Tuberculosis using [^{18}F]2-Fluoro-Deoxy-D-Glucose Positron Emission Tomography and Computed Tomography. Antimicrob Agents Chemother 56:4391-4402, 2012
65. Lin PL, Maiello P, Gideon HP, et al: PET CT Identifies Reactivation Risk in Cynomolgus Macaques with Latent M. tuberculosis. PLoS Pathog 12:e1005739, 2016
66. Lin PL, Myers A, Smith L, et al: Tumor necrosis factor neutralization results in disseminated disease in acute and latent Mycobacterium tuberculosis infection with normal granuloma structure in a cynomolgus macaque model. Arthritis Rheum 62:340-350, 2010
67. Chen RY, Yu X, Smith B, et al: Radiological and functional evidence of the bronchial spread of tuberculosis: an observational analysis. Lancet Microbe 2:e518-e526, 2021
68. Cadena AM, Fortune SM, Flynn JL: Heterogeneity in tuberculosis. Nat Rev Immunol 17:691-702, 2017
69. Esmail H, Lai RP, Lesosky M, et al: Characterization of progressive HIV-associated tuberculosis using 2-deoxy-2-[^{18}F]fluoro-D-glucose positron emission and computed tomography. Nat Med 22:1090-1093, 2016
70. Fox W: Whither short-course chemotherapy? Br J Dis Chest 75:331-357, 1981
71. Gillespie SH, Crook AM, McHugh TD, et al: Four-month moxifloxacin-based regimens for drug-sensitive tuberculosis. N Engl J Med 371:1577‑1587, 2014
72. Merle CS, Fielding K, Sow OB, et al: OFLOTUB/Gatifloxacin for Tuberculosis Project, A four-month gatifloxacin-containing regimen for treating tuberculosis. N Engl J Med 371:1588‑1598, 2014
73. Wallis RS, Kim P, Cole S, et al: Tuberculosis biomarkers discovery: developments, needs, and challenges. Lancet Infect Dis 13:362-372, 2013
74. Phillips PP, Fielding K, Nunn AJ. An evaluation of culture results during treatment for tuberculosis as surrogate endpoints for treatment failure and relapse. PLoS One 8:e63840, 2013
75. Horne DJ, Royce SE, Gooze L, et al: Sputum monitoring during tuberculosis treatment for predicting outcome: systematic review and meta-analysis. Lancet Infect Dis 10:387–394, 2010

76. Chen RY, Dodd LE, Lee M, et al: PET/CT and High Resolution CT as potential imaging biomarkers associated with treatment outcomes in MDR-TB. Sci Transl Med 6:265ra166, 2014
77. Davis SL, Nuermberger EL, Um PK, et al: Noninvasive Pulmonary [18F]-2-Fluoro-Deoxy-D-Glucose Positron Emission Tomography Correlates with Bactericidal Activity of Tuberculosis Drug Treatment. Antimicrob Agents Chemother 53:4879-4884, 2009
78. Lin PL, Coleman T, Carney JPJ, et al: Radiologic Responses in Cynomolgus Macaques for Assessing Tuberculosis Chemotherapy Regimens. Antimicrob Agents Chemother 57:4237-4244, 2013
79. Coleman MT, Chen RY, Lee M, et al: PET/CT demonstrates a therapeutic response to oxazolidinones in *Mycobacterium tuberculosis*-infected macaques and humans. Sci Transl Med 6:265ra167, 2014
80. Xie YL, de Jager VR, Chen RY, et al: Fourteen-day PET/CT imaging to monitor drug combination activity in treated individuals with tuberculosis. Sci Transl Med 13:eabd7618, 2021
81. Manzardo C, Guardo AC, Letang E, et al: Opportunistic infections and immune reconstitution inflammatory syndrome in HIV-1-infected adults in the combined antiretroviral therapy era: a comprehensive review. Expert Rev Anti Infect Ther 13:751-767, 2015
82. Lawal IO, Orunmuyi AT, Popoola GO, et al: Immune reconstitution inflammatory syndrome-associated Graves disease in HIV-infected patients: clinical characteristics and response to radioactive iodine therapy. HIV Med 22:907-916, 2021
83. Worodria W, Menten J, Massinga-Loembe M, et al: Clinical spectrum, risk factors and outcome of immune reconstitution inflammatory syndrome in patients with tuberculosis-INV coinfection. Antivir Ther 17:841-848, 2012
84. Hammoud DA, Bolougoura A, Papadakis GZ, et al: Increased Metabolic Activity on 18F-Fluorodeoxyglucose Positron Emission Tomography-Computed Tomography in Human Immunodeficiency Virus-Associated Immune Reconstitution Inflammatory Syndrome. Clin Infect Dis 68:229-238, 2019
85. Sood A, Mittal BR, Modi M, et al: ^{18}F-FDG PET/CT in Tuberculosis: Can Interim PET/CT Predict the Clinical Outcome of Patients? Clin Nucl Med 45:276-282, 2020
86. Sandra-Mantel L, Kaoutar J, Alfaiate T, et al: [^{18}F]FDG Positron Emission Tomography for Initial Staging and Healing Assessment at the End of Therapy in Lymph Nodes and Bone Tuberculosis. Front Med 8:715115, 2021
87. Lang D, Huber H, Kaiser B, et al: SUV as a Possible Predictor of Disease Extent and Therapy Duration in Complex Tuberculosis. Clin Nucl Med 43:94-100, 2018
88. Sánchez-Montalviá A, Barios M, Salvador F, et al: Usefulness of FDG PET/CT in the management of tuberculosis. PLoS ONE 14:e0221516, 2019
89. Bomanji J, Sharma R, Mittal BR et al: Sequential ^{18}F-fluorodeoxyglucose positron emission tomography (^{18}F-FDG PET) scan findings in patients with extrapulmonary tuberculosis during the course of treatment – a prospective observational study. Eur J Nucl Med Mol Imaging 47:3118-3129, 2020
90. Sathekge M, Maes A, Kgomo M, et al: Use of 18F-FDG PET to Predict Response to First-Line Tuberculostatics in HIV-Associated Tuberculosis. J Nucl Med 52:880-886, 2011
91. Sathekge M, Maes A, D'Asseler Y, et al: Tuberculous lymphadenitis: FDG PET and CT findings in responsive and nonresponsive disease. Eur J Nucl Med Mol Imaging 39:1184-1190, 2012
92. Singh A, Tripathi M, Kodan P, et al: Positron-emission-tomography in tubercular lymphadenopathy: A study of its role in evaluating post-treatment response. Drug Discov Ther 2021

93. Lefebvre N, Argemi X, Meyer N, et al: Clinical usefulness of ^{18}F-FDG PET/CT for initial staging and assessment of treatment efficacy in patients with lymph node tuberculosis. Nucl Med and Biology 50:17-24, 2017
94. Vanino E, Tadolini M, Evangelisti G, et al: Spinal tuberculosis: proposed spinal infection multidisciplinary management project (SIMP) flow chart revision. Eur Red Med Pharmacol Sci 24:1428-1434, 2020
95. Mann TN, Warwick J, Chegou NN, et al: Biomarkers to predict FDG PET/CT activity after the standard duration of treatment for spinal tuberculosis: An exploratory study. Tuberculosis 129:102107, 2021
96. Dureja S, Sen IB, Acharya S: Potential role of F18 FDG PET-CT as an imaging biomarker for the noninvasive evaluation in uncomplicated skeletal tuberculosis: a prospective clinical observational study. Eur Spine 23:2449-2454, 2014
97. Mittal S, Jain AK, Chakraborti KL, et al: Evaluation of healed status in tuberculosis of spine by fluorodeoxyglucose-positron emission tomography/computed tomography and contrast magnetic resonance imaging. Indian J Orthop 53:160-168, 2019
98. Goyal D, Shriwastav R, Mittal R, et al: Role of ^{18}F-FDG PET/CT in the Assessment of Response to Antitubercular Chemotherapy and Identification of Treatment Endpoint in Patients with Tuberculosis of the Joints: A Pilot Study. Clin Nucl Med 46:449-455, 2021
99. Gambhir S, Kumar M, Ravina M, et al: Role of ^{18}F-FDG PET in demonstrating disease burden in patients with tuberculous meningitis. J Neurol Sci 370:196-200, 2016
100. Nigam H, Gambhir S, Pandey S, et al: 18FDG-Positron Emission Tomography in Patients with Tuberculous Meningitis: A Prospective Evaluation. Am J Trop Med Hyg 105:1038-1041, 2021
101. Maramattom BV, Santhamma SGN: Tuberculous Encephalitis may be undetectable on magnetic resonance imaging but detectable on 18F-fluorodeoxyglucose positron emission tomography-computed tomography. Am J Trop Med Hyg 105:1031-1037, 2021
102. Jain A, Goyal MK, Mittal BR et al: 18FDG-PET is sensitive tool for detection of extracranial tuberculous foci in central nervous system tuberculosis-Preliminary observations from a tertiary care center in northern India. J Neurol Sci 409:116585, 2020
103. Lawal IO, Stoltz AC, Sathekge MM: Molecular imaging of cardiovascular inflammation and infection in people living with HIV infection. Clin Transl Imaging 8:141-155, 2020
104. Hyeon CW, Yi HK, Kim EK, et al: The role of 18F-fluorodeoxyglucose-positron emission tomography/computed tomography in the differential diagnosis of pericardial disease. Sci Rep 10:21524, 2020
105. Dong A, Dong H, Wang Y, et al: (18)F-FDG PET/CT in differentiating acute tuberculous from idiopathic pericarditis: preliminary study. Clin Nucl Med 38:e160-e165, 2013
106. Ozmen O, Koksal D, Ozcan A, et al: Decreased metabolic uptake in tuberculous pericarditis indicating response to antituberculous therapy on FDG PET/CT. Clin Nucl Med 39:917-919, 2014
107. Lawal I, Sathekge M: F-18 FDG PET/CT imaging of cardiac and vascular inflammation and infection. Br Med Bull 120:55-74, 2016
108. Lawal IO, Fourie BP, Mathebula M, et al: 18F-FDG PET/CT as a Noninvasive Biomarker for Assessing Adequacy of Treatment and Predicting Relapse in Patients Treated for Pulmonary Tuberculosis. J Nucl Med 61:412-417, 2020

109. Malherbe ST, Shenai S, Ronacher K, et al: Persisting positron emission tomography lesion activity and Mycobacterium tuberculosis mRNA after tuberculosis cure. Nat Med 22:1094-1100, 2016
110. Lawal IO, Mokoala KMG, Mathebula M, et al: Correlation Between CT features of Active Tuberculosis and Residual Metabolic Activity on End-of-Treatment FDG PET/CT in Patients Treated for Pulmonary Tuberculosis. Front Med 9:791653, 2022
111. Beltran CGG, Heunis T, Gallant J, et al: Investigating Non-sterilizing Cure in TB Patients at the End of Successful Anti-TB Therapy. Front Cell Infect Microbiol 10:443, 2020
112. Thompson EG, Du Y, Malherbe S, et al: Host blood RNA signatures predict the outcome of tuberculosis treatment. Tuberculosis 107:48-58, 2017
113. Horsburgh CR, Barry CE, Lange C: Treatment of Tuberculosis. N Engl J Med 373:2149-2160, 2015
114. Sritharan M: Iron Homeostasis and Mycobacterium tuberculosis: Mechanistic Insights into Siderophore-Mediated Iron Uptake. J Bacteriol 198:2399-2409, 2016
115. Boelaert JR, Vandecasteele SJ, Appelberg R, et al: The effect of the host's iron status on tuberculosis. I Infect Dis 195:1745-1753, 2007
116. Nevitt, T: War-Fe-re: iron at the core of fungal virulence and host immunity. Biometals 24:547-558, 2011
117. Baatjies L, Loxton AG, Williams MJ: Host and bacterial Iron Homeostasis, an Underexplored Area in Tuberculosis Biomarker Research. Front Immunol 12:742059, 2021
118. Walsh TJ, Bekerman C, Chausow A, et al: The value of gallium-67 scanning in pulmonary tuberculosis. Am Rev Respir Dis 132:746-747, 1985
119. Liu SF, Liu JW, Lin MC, et al: Monitoring treatment responses in patients with pulmonary TB using serial lung gallium-67 scintigraphy. AJR Am J Roentgenol 188:W403-W408, 2007
120. Vorster M, Maes A, van de Wiele C, et al: ^{68}Ga-citrate PET/CT in tuberculosis. A pilot study. Q J Nucl Med Mol Imaging 63:48-55, 2019
121. Vorster M, Maes A, Jacobs A, et al: Evaluating the possible role of ^{68}Ga-citrate PET/CT in the characterization of indeterminate lung lesions. Ann Nucl Med 28:523-530, 2014
122. Ankrah AO, Lawal IO, Boshomane TMG, et al: Comparison of Fluorine(18)-fluorodeoxyglucose and Gallium(68)-citrate PET/CT in patients with tuberculosis. Nuklearmedizin 58:371-378, 2019
123. Lawal IO, Ololade KO, Lengana T, et al: Gallium-68-dotate PET/CT is better than CT in the management of somatostatin expressing tumors: First experience in Africa. Hell J Nucl Med 20:128-133, 2017
124. Barrio M, Czernin J, Fanti S, et al: The Impact of Somatostatin Receptor-Directed PET/CT on the Management of Patients with Neuroendocrine Tumor: A Systematic Review and Meta-Analysis. J Nucl Med 58:756-761, 2017
125. Naftalin CM, Leek F, Hallinan JTPD, et al: Comparison of68Ga-DOTATOC with 18F-FDG using PET/MRI imaging in patients with pulmonary tuberculosis. Sci Rep 10:14236, 2020
126. Rosado-de-Castro PH, Pereira-de-Carvelho T, Barreto MM, et al: Comparison of 68Ga-DOTATOC and 18F-FDG Thoracic Lymph Node and Pulmonary Lesion Uptake Using PET/CT in Postprimary Tuberculosis. Am J Trop Med Hyg 106:1340-1344, 2022
127. D'Souza MM, Sharma R, Jaimini A, et al: Metabolic assessment of intracranial tuberculoma using ^{11}C-methionine and ^{18}F-FDG PET/CT. Nucl Med Commun 33:408-414, 2012

128. Tsao CH, Wu CY, Chang CW, et al: Micro-PET imaging of [^{18}F]fluoroacetate combined with [^{18}F]FDG to differentiate chronic *Mycobacterium tuberculosis* infection from an acute bacterial infection in a mouse model: a preliminary study. Nucl Med Commun 40:639-644, 2019
129. Rundell SR, Wagar ZL, Meints LM, et al: Deoxyfluoro-D-trehalose (FDTre) analogues as potential PET probes for imaging mycobacterial infection: rapid synthsis and purification, conformational analysis, and uptake by mycobacteria. Org Biomol Chem 14:8598-8609, 2016
130. Peña-Zalbidea S, Huang AY, Kavunja HW, et al: Chemoenzymatic radiosynthesis of 2-deoxy-2-[^{18}F]fluoro-d-trehalose ([^{18}F]-2-FDTre): A PET radioprobe for in vivo tracing of trehalose metabolism. Carbohydr Res 472:16-22, 2019
131. Gideon HP, Phuah J, Junecko BA, et al: Neutrophils express pro- and anti-inflammatory cytokines in granulomas from Mycobacterium tuberculosis-infected cynomolgus macaques. Mucosal Immunol 12:1370-1381, 2019
132. Hult C, Mattila JT, Gideon HP, et al: Neutrophil Dynamics Affect *Mycobacterium tuberculosis* Granuloma Outcomes and Dissemination. Front Immunol 12:712457, 2021
133. Lawal IO, Gheysens O, Sathekge MM et al: Editorial: Functional Imaging of Inflammation and Infection. Front Med 9:925635, 2022
134. More S, Marakalala MJ, Sathekge M: Tuberculosis: Role of Nuclear Medicine and Molecular Imaging with Potential Impact of Neutrophil-Specific Tracers. Fron Med 8:758636, 2021
135. Mattila JT, Beaino W, Maiello P, et al: Positron Emission Tomography Imaging of Macaques with Tuberculosis Identifies Temporal Changes in Granuloma Glucose Metabolism and Integrin α4β1-Expressing Immune Cells. J Immunol 199:806-815, 2017
136. Mattila JT, Beaino W, White AG, et al: Retention of ^{64}Cu-FLFLF, a Formyl Peptide Receptor 1-Specific PET Probe, Correlates with Macrophage and Neutrophil Abundance in Lung Granulomas from Cynomolgus Macaques. ACS Infect Dis 7:2264-2276, 2021
137. Hunter L, Hingley-Wilson S, Stewart GR, et al: Dynamics of Macrophage, T and B Cell Infiltration Within Pulmonary Granulomas Induced by Mycobacterium tuberculosis in two Non-Human Primate Models of Aerosol Infection. Front Immunol 12:776913, 2022
138. Urbanowski ME, Ordonez AA, Ruiz-Bedoya CA, et al: Cavitary tuberculosis: the gateway of disease transmission. Lancet Infect Dis 20:e117-e128, 2020
139. Via LE, Lin PL, Ray SM, et al: Tuberculous granulomas are hypoxic in guinea pigs, rabbits, and nonhuman primates. Infect Immun 76:2333-2340, 2008
140. Vandiviere HM, Loring WE, Melvin I, et al: The treated pulmonary lesion and its tubercle bacillus. II. The death and resurrection. Am J Med Sci 232:30-37, 1956
141. Russel DG, VanderVen BC, Lee W, et al: *Mycobacterium tuberculosis* Wears What It eats. Cell Host Microbe 8:68-76, 2010
142. Belton M, Brilha S, Manavaki R, et al: Hypoxia and tissue destruction in pulmonary TB. Thorax 71:1145-1153, 2016
143. Mokoala KMG, Lawal IO, Jeong JM, et al: Radionuclide imaging of hypoxia: Whare are we now? Special attention to cancer of the cervix uteri. Hell J Nucl Med 24:247-261, 2021
144. Bresser PL, Vorster M, Sathekge MM: An overview of the developments and potential applications of ^{68}Ga-labelled PET/CT hypoxia imaging. Ann Nucl Med 35:148-158, 2021
145. Mokoala KMG, Lawal IO, Maserumule L, et al: A Prospective Investigation of Tumor Hypoxia Imaging with ^{68}Ga-Nitroimidazole PET/CT in Patients with Carcinoma of the Cervix

Uteri and Comparison with ^{18}F-FDG PET/CT: Correlation with Immunohistochemistry. J Clin Med 11:962, 2022
146. Bresser PL, Sathekge MM, Vorster M: PET/CT features of a novel gallium-68 labelled hypoxia seeking agent in patients diagnosed with tuberculosis: a proof-of-concept study. Nucl Med Commun (Epub ahead of print)
147. Polena H, Boudou F, Tilleul S, et al: Mycobacterium tuberculosis exploits the formation of new blood vessels for its dissemination. Sci Rep 6:33162, 2016
148. Kang F, Wang S, Tian F, et al: Comparing the Diagnostic Potential of ^{68}Ga-Alfatide II and ^{18}F-FDG in Differentiating Between Non-Small Cell Lung Cancer and Tuberculosis. J Nucl Med 57:672-677, 2016
149. Du X, Zhang Y, Chen L, et al: Comparing the Differential Values of 18F-Alfatide II PET/CT between Tuberculosis and Lung Cancer patients. Contrast Media Mol Imaging 2018:8194678, 2018
150. de Galiza Barbosa F, Queiroz MA, Nunes RF, et al: Nonprostatic diseases on PSMA PET imaging: a spectrum of benign and malignant findings. Cancer Imaging 20:23, 2020
151. Pyka T, Weirich G, Einspieler I, et al: 68Ga-PSMA-HBED-CC PET for Differential Diagnosis of Suggestive Lung Lesions in Patients with Prostate Cancer. J Nucl Med 57:367-371, 2016
152. Liu H, Liu Y, Chen Y, et al: 68Ga-PSMA Uptake in Pulmonary Tuberculosis: A Pitfall in Prostate cancer PET Imaging. Nuklearmedizin 60:252-253, 2021
153. Gupta N, Elumalai RK, Verma R, et al: Spinal Tuberculosis Mimicking as Prostate Cancer Metastases in Ga-68 Prostate-specific Membrane Antigen Positron-emission Tomography/Computed Tomography. Indian J Nucl Med 35:271-273, 2020
154. Wong VCK, Shen L, Nasser E, et al: 68Ga-Prostate-Specific Membrane Antigen Uptake in Cerebral Tuberculosis. Clin Nucl Med 45:238-240, 2020
155. Bohil A, Seshadri N, Rathi N, et al: Tubercular Spondylitis: A Rare Complication of BCGosis Masquerading as Metastasis on 18F-PSMA-1007 PET/CT. Clin Nucl Med 47:e254-e256, 2022
156. Warsinske HC, DiFazio RM, Linderman JJ, et al: Identifying mechanisms driving formation of granuloma-associated fibrosis during Mycobacterium tuberculosis infection. J Theor Biol 429:1-17, 2017
157. Kratochwil C, Flechsig P, Lindner T, et al: ^{68}Ga-FAPI PET/CT: Tracer Uptake in 28 Different Kinds of Cancer. J Nucl Med 60:801-805, 2019
158. Dendl K, Koerber SA, Finck R, et al: ^{68}Ga-FAPI-PET/CT in patients with various gynecological malignancies. Eur J Nucl Med Mol Imaging 48:4089-4100, 2021
159. Novruzov E, Dendl K, Ndlovu H, et al: Head-to-head Intra-individual Comparison of [^{68}Ga]-FAPI and [^{18}F]-FDG PET/CT in Patients with Bladder Cancer. Mol Imaging Biol (Epub ahead of print)
160. Deng Y, Wu J, Xu C, et al: Primary Solitary Tuberculosis in the Hepatic Round Ligament Detected by 68Ga-FAPI PET/CT. Clin Nucl Med 47:e414-e416, 2022
161. Zheng J, Lin K, Zheng S, et al: 68Ga-FAPI and 18F-PET/CT Images in Intestinal Tuberculosis. Clin Nucl Med 47:239-240, 2022
162. Ordonez AA, Tucker EW, Anderson CJ, et al: Visualizing the dynamics of tuberculosis pathology using molecular imaging. J Clin Invest 131:e145107, 2021
163. Dheda K, Lenders L, Magombedze G, et al: Drug-Penetration Gradients Associated with Acquired Drug Resistance in Patients with Tuberculosis. Am J Respir Crit Care Med 198:1208-1219, 2018

164. Gordon O, Ruiz-Bedoya CA, Ordonez AA, et al: Molecular Imaging: a Novel Tool To Visualize Pathogenesis of Infections *In Situ*. mBio 10:e00317-19, 2019
165. DeMarco VP, Ordonez AA, Klunk M, et al: Determination of [^{11}C]Rifampin Pharmacokinetics within *Mycobacterium tuberculosis*-Infected Mice by Using Dynamic Positron Emission Tomography Bioimaging. Antimicrob Agents Chemother 59:5768-5774, 2015
166. Weinstein EA, Liu L, Ordonez AA, et al: Noninvasive Determination of 2-[^{18}F]-Fluoroisonicotinic Acid Hydrazide Pharmacokinetics by Positron Emission Tomography in *Mycobacterium tuberculosis*-Infected Mice. Antimicrob Agents Chemother 56:6284-6290, 2012
167. Zhang Z, Ordonez AA, Smith-Jones P, et al: The biodistribution of 5-[^{18}F] fluoropyrazinamide in *Mycobacterium tuberculosis*-infected mice determined by positron emission tomography. PLoS ONE 12:e0170871, 2017
168. Ordonez AA, Carroll LS, Abhisshek S, et al: Radiosynthesis and PET Bioimaging of ^{76}Br-Bedaquiline in a Murine Model of Tuberculosis. ACS Infect Dis 5:1996-2002, 2019
169. Mota F, Jadhav R, Ruiz-Bedoya CA, et al: Radiosynthesis and Biodistribution of ^{18}F-Linezolid in *Mycobacterium tuberculosis*-Infected Mice Using Positron Emission Tomography. ACS Infect Dis 6:916-921, 2020
170. Ordonez AA, Wang H, Magombedze G, et al: Dynamic imaging in patients with tuberculosis reveals heterogenous drug exposures in pulmonary lesions. Nat Med 26:s29-s34, 2020
171. Ruiz-Bedoya CA, Mota F, Tucker EW, et al: High-dose rifampin improves bactericidal activity without increased intracerebral inflammation in animal models of tuberculous meningitis. J Clin Invest 132:e155851, 2022
172. Tucker EW, Guglieri-Lopez B, Ordonez AA, et al. Noninvasive ^{11}C-rifampin positron emission tomography reveals drug biodistribution in tuberculous meningitis. Sci Transl Med 10:eaau965, 2019